

# Structure and Dynamic Exchange in Rhodium $\eta^2$ -Naphthalene and Rhodium $\eta^2$ -Phenanthrene Complexes: Quantitative NOESY and EXSY Studies

Leroy Cronin, Catherine L. Higgitt, and Robin N. Perutz\*

Department of Chemistry, University of York, York YO10 5DD, U.K.

Received October 19, 1999

Complexes of naphthalene and phenanthrene with rhodium( $\eta^5$ -cyclopentadienyl)(trimethylphosphine) have been studied by quantitative two-dimensional nuclear Overhauser (NOESY) and exchange spectroscopy (EXSY). Naphthalene coordinates in the  $\eta^2$ -1,2-mode as  $(\eta^5\text{-C}_5\text{H}_5)\text{Rh}(\text{PMe}_3)(\eta^2\text{-C}_{10}\text{H}_8)$ . At 260 K, NOESY peaks establish that the solution conformer has the hydrogen atoms on the coordinated double bond bent out of the arene plane toward the  $\text{PMe}_3$  ligand. The effective average distance,  $r_{\text{eff}}$ , of these hydrogen atoms from those in the  $\text{PMe}_3$  ligand is calculated as 3.52 Å by matrix analysis of the NOESY spectrum. At room temperature,  $(\eta^5\text{-C}_5\text{H}_5)\text{Rh}(\text{PMe}_3)(\eta^2\text{-C}_{10}\text{H}_8)$  undergoes an intramolecular [1,3]-metallotropic shift within the coordinated ring with  $\Delta G^\ddagger_{300}$  of 74.4 kJ mol<sup>-1</sup> detected by EXSY spectroscopy. This species is in equilibrium (a) with the C–H activated isomer  $(\eta^5\text{-C}_5\text{H}_5)\text{Rh}(\text{PMe}_3)(\text{C}_{10}\text{H}_7)\text{H}$  and (b) with the dinuclear complex  $[(\eta^5\text{-C}_5\text{H}_5)\text{Rh}(\text{PMe}_3)]_2(\mu\text{-}1,2\text{-}\eta^2\text{-}3,4\text{-}\eta^2\text{-C}_{10}\text{H}_8)$  and free naphthalene. The free energy change at 300 K for conversion of  $(\eta^5\text{-C}_5\text{H}_5)\text{Rh}(\text{PMe}_3)(\eta^2\text{-C}_{10}\text{H}_8)$  to  $(\eta^5\text{-C}_5\text{H}_5)\text{Rh}(\text{PMe}_3)(\text{C}_{10}\text{H}_7)\text{H}$  is +11.5 kJ mol<sup>-1</sup> compared to +2.2 kJ mol<sup>-1</sup> for the  $(\eta^5\text{-C}_5\text{Me}_5)$  analogue. The crystal structure of the dinuclear complex,  $[(\eta^5\text{-C}_5\text{H}_5)\text{Rh}(\text{PMe}_3)]_2(\mu\text{-}1,2\text{-}\eta^2\text{-}3,4\text{-}\eta^2\text{-C}_{10}\text{H}_8)$ , shows that this molecule adopts the structure with the two rhodium centers coordinated antifacially to the same ring of the naphthalene ligand. The C–C bond lengths of the coordinated ring show conspicuous alternation, while those of the uncoordinated ring differ less than those in free naphthalene. The mean separation of the hydrogen atoms attached to the coordinated C=C bond from the  $\text{PMe}_3$  hydrogen atoms, averaged from the crystal structure as  $1/\langle r^{-3} \rangle^{1/3}$  for each independent rhodium center, is 3.56 Å, compared to 3.48 Å for  $r_{\text{eff}}$  measured in solution by NOESY spectroscopy. The phenanthrene complex  $(\eta^5\text{-C}_5\text{H}_5)\text{Rh}(\text{PMe}_3)(\eta^2\text{-}9,10\text{-C}_{14}\text{H}_{10})$  adopts a conformation similar to the naphthalene complex; the value of  $r_{\text{eff}}$  is estimated to be reduced to 3.43 Å.

## Introduction

**NOESY and EXSY Spectroscopy.** Nuclear Overhauser spectroscopy (NOESY)<sup>1–3</sup> has found extensive application in organometallic chemistry as a means of determining molecular conformations in solution, especially when crystal structures cannot be obtained.<sup>4</sup> Most applications make qualitative use of the NOESY data, but the method can give quantitative distance information if there is a rigid portion of the structure of known geometry that can be used for calibration. To simplify the analysis, the complex should have a rigid conformation and a reasonably simple NMR spectrum and should show only weak scalar coupling between the nuclei of interest. Examples of the qualitative applications of NOESY include Pregosin's studies of allyl binding in chiral palladium complexes and his demonstration of

PtHN interactions in platinum aryl complexes.<sup>4,5</sup> A more quantitative approach has been taken by Field, Messerle, et al., who have used the ratios of NOESY cross-peak integrals to obtain ratios of internuclear distances in lithium alkenyls.<sup>6</sup> Cross-relaxation rates fall off with the inverse sixth power of internuclear distance. If several equivalent nuclei undergo internal rotation (e.g., a methyl group), the set of internuclear distances,  $r_i$ , can be approximated by a single effective distance,  $r_{\text{eff}}$ , where  $r_{\text{eff}} \approx 1/\langle r_i^{-3} \rangle^{1/3}$  and  $r_{\text{eff}}^{-6} \approx \langle r_i^{-3} \rangle^2$ .<sup>1,7</sup> In a simple rigid system, NOESY cross-peaks are not detected beyond ca. 3 Å, but this limit may be extended slightly in complex systems where the effects of several nuclei are averaged.

Exchange spectroscopy (EXSY) is a suitable method for investigating slow exchange processes and determin-

(1) (a) Neuhaus, D.; Williamson, M. *The Nuclear Overhauser Effect in Structural and Conformational Analysis*; VCH: New York, 1989. (b) Macura, S.; Ernst, R. R. *Mol. Phys.* **1980**, *41*, 95.

(2) Freeman, R. *A Handbook of Nuclear Magnetic Resonance*; Longmans: Harlow, U.K., 1988.

(3) Günther, H. *NMR Spectroscopy: Basic Principles, Concepts and Applications in Chemistry*, 2nd ed.; Wiley: Chichester, U.K., 1995.

(4) Pregosin, P. S.; Salzmann, R. *Coord. Chem. Rev.* **1996**, *155*, 35. Pregosin, P. S.; Ammann, C. *Pure Appl. Chem.* **1989**, *61*, 1771.

(5) Albinati, A.; Ammann, C.; Pregosin, P. S.; Rügger, H. *Organometallics* **1990**, *9*, 1826. Drommi, D.; Nesper, R.; Pregosin, P. S.; Trabesinger, G.; Zürcher, F. *Organometallics* **1997**, *16*, 4268. Pregosin, P. S.; Rügger, H.; Wombacher, F.; van Koten, G.; Grove, D. M.; Wehman-Ooyevaar, I. C. M. *Magn. Reson. Chem.* **1992**, *30*, 548.

(6) Field, L. D.; Gardiner, M. G.; Messerle, B. A.; Raston, C. L. *Organometallics* **1992**, *11*, 3566.

(7) Pegg, D. T.; Bendall, M. R.; Doddrell, D. M. *Aust. J. Chem.* **1980**, *33*, 1167.

ing the rates of exchange.<sup>1,8–11</sup> It is very useful for distinguishing intra- and intermolecular exchange processes and mapping out exchange networks. EXSY and NOESY cross-peaks are determined in the same experiment; for small molecules with short correlation times, NOESY cross-peaks are negative if the diagonal peaks are phased as positive, whereas EXSY cross-peaks are positive. Comparisons have been made between several of the methods of analyzing the EXSY data, and the full matrix approach has proved to be the most successful for extracting quantitative rate information.<sup>12–14</sup> There are numerous examples of applications of EXSY in transition metal chemistry including studies of sulfur inversion at platinum thioether complexes,<sup>14</sup> exchange of coordinated and uncoordinated carbon atoms in cobalt cycloheptatriene complexes,<sup>15</sup> and migration of a metal over the surface of the fullerene in metal( $\eta^2$ -C<sub>60</sub>) complexes.<sup>16</sup> We have shown previously how <sup>19</sup>F–<sup>19</sup>F EXSY reveals the ring hopping of ( $\eta^5$ -C<sub>5</sub>H<sub>5</sub>)Re(CO)<sub>2</sub>( $\eta^2$ -C<sub>6</sub>F<sub>6</sub>).<sup>17</sup>

**( $\eta^5$ -C<sub>5</sub>R<sub>5</sub>)Rh(PMe<sub>3</sub>)( $\eta^2$ -arene) (R = H, Me) Complexes.** There is abundant evidence that oxidative addition of arenes (C–H bond activation) at cyclopentadienyl rhodium proceeds via  $\eta^2$ -precoordination of the arene.<sup>18–20</sup> X-ray crystal structures of complexes of  $\eta^2$ -coordinated arenes (or fluoroarenes) indicate that the hydrogen (or fluorine) atoms attached to the coordinated carbon atoms are bent out of the plane of the arene ring.<sup>17–19,21–23</sup> Where a cyclopentadienyl group is present as an additional ligand, these hydrogen atoms on the

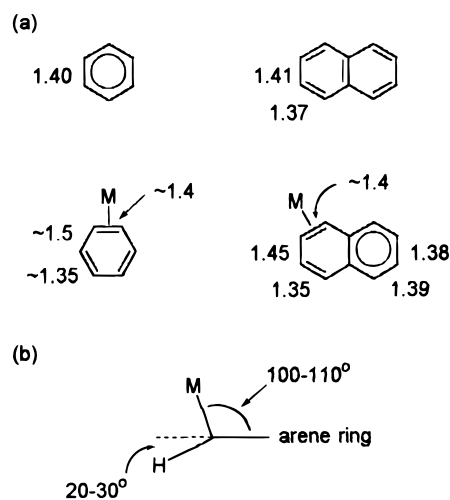
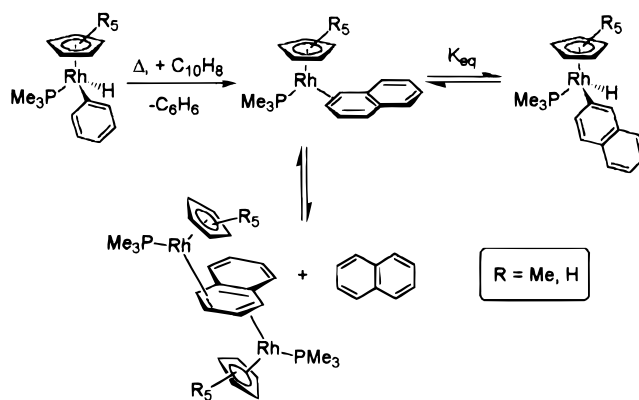


**Figure 1.** Summary of the distortions to the arene upon  $\eta^2$ -coordination to a metal center.<sup>17–24</sup> (a) distances/Å, (b) angles.

**Scheme 1. Reactivity of ( $\eta^5$ -C<sub>5</sub>R<sub>5</sub>)Rh(PMe<sub>3</sub>)(C<sub>6</sub>H<sub>5</sub>)H toward Naphthalene (R = Me,  $K_{eq}$  = 0.5 from ref 18, 20; R = H,  $K_{eq}$  = 0.01, this work)**



arene ring are bent away from the  $\eta^5$ -C<sub>5</sub>H<sub>5</sub> or  $\eta^5$ -C<sub>5</sub>Me<sub>5</sub> ligand. Theoretical calculations and X-ray crystal data show that  $\eta^2$ -coordination causes deconjugation of the arene rings in polycyclic arenes and alteration of the arene bond lengths consistent with the localization of  $\pi$  electron density.<sup>23–25</sup> Figure 1 summarizes the distortions observed upon  $\eta^2$ -coordination of an arene or of naphthalene to a metal complex.

In one of the most revealing approaches to studying the relation between  $\eta^2$ -arene complexes and C–H bond activation, equilibria have been set up between the two types of complex. One such equilibrium is that between ( $\eta^5$ -C<sub>5</sub>Me<sub>5</sub>)Rh(PMe<sub>3</sub>)( $\eta^2$ -1,2-C<sub>10</sub>H<sub>8</sub>) and ( $\eta^5$ -C<sub>5</sub>Me<sub>5</sub>)Rh(PMe<sub>3</sub>)(C<sub>10</sub>H<sub>7</sub>)H (C<sub>10</sub>H<sub>8</sub> = naphthalene, Scheme 1).<sup>19,20</sup> Removal of naphthalene from this system leads to the formation of a binuclear species, [( $\eta^5$ -C<sub>5</sub>Me<sub>5</sub>)Rh(PMe<sub>3</sub>)]<sub>2</sub>( $\mu$ -1,2- $\eta^2$ -3,4- $\eta^2$ -C<sub>10</sub>H<sub>8</sub>), also at equilibrium, for which an X-ray crystal structure is known (Scheme 1).<sup>19,23</sup> For the analogous  $\eta^5$ -C<sub>5</sub>H<sub>5</sub> system, it appeared that the thermal reaction of ( $\eta^5$ -C<sub>5</sub>H<sub>5</sub>)Rh(PMe<sub>3</sub>)(C<sub>6</sub>H<sub>5</sub>)H with naphthalene

(8) Orrell, K. G.; Šik, V. *Annu. Rep. NMR Spectrosc.* **1987**, 19. Willem, R. *Prog. Nucl. Magn. Reson. Spectrosc.* **1987**, 20, 1.

(9) Ernst, R. R.; Bodenhausen, G.; Wokaun, A. *Principles of Nuclear Magnetic Resonance in One and Two Dimensions*; Oxford University Press: New York, 1987.

(10) Perrin, C. L.; Dwyer, T. *J. Chem. Rev.* **1990**, 90, 935.

(11) Mann, B. E. In *Encyclopedia of Nuclear Magnetic Resonance*; Grant, D. M., Harris, R. K., Eds.; Wiley: Chichester, U.K., 1996; Vol. 5, p 3400. Orrell, K. G. *Ibid.* Vol. 3, p 2071. Orrell, K. G. *Ibid.* Vol. 8, p 4850.

(12) Borgias, B. A.; Gochin, M.; Kerwood, D. J.; James, T. L. *Prog. Nucl. Magn. Reson. Spectrosc.* **1990**, 22, 83.

(13) Perrin, C. L.; Gipe, R. K. *J. Am. Chem. Soc.* **1984**, 106, 4036.

(14) Abel, E. W.; Coston, T. P. J.; Orrell, K. G.; Šik, V.; Stephenson, D. *J. Magn. Reson.*, **1986**, 70, 34.

(15) Benn, R.; Cibura, K.; Hofmann, P.; Jonas, K.; Rufinska, A. *Organometallics* **1985**, 4, 2214.

(16) Green, M. L. H.; Stephens, A. H. *Chem. Commun.* **1997**, 793.

(17) Higgitt, C. L.; Klahn, A. H.; Moore, M. H.; Oelckers, B.; Partridge, M. G.; Perutz, R. N. *J. Chem. Soc., Dalton Trans.* **1997**, 1269.

(18) Belt, S. T.; Duckett, S. B.; Helliwell, M.; Perutz, R. N. *J. Chem. Soc., Chem. Commun.* **1989**, 928. Belt, S. T.; Dong, L.; Duckett, S. B.; Jones, W. D.; Partridge, M. G.; Perutz, R. N. *J. Chem. Soc., Chem. Commun.* **1991**, 266. Jones, W. D.; Feher, F. J. *J. Am. Chem. Soc.* **1982**, 104, 4240. Jones, W. D.; Feher, F. J. *J. Am. Chem. Soc.* **1984**, 106, 1650. Jones, W. D.; Feher, F. J. *Acc. Chem. Res.* **1989**, 22, 91. Jones, W. D.; Feher, F. J. *J. Am. Chem. Soc.* **1986**, 108, 4814.

(19) Jones, W. D.; Dong, L. *J. Am. Chem. Soc.* **1989**, 111, 8722.

(20) Chin, R. M.; Dong, L.; Duckett, S. B.; Partridge, M. G.; Jones, W. D.; Perutz, R. N. *J. Am. Chem. Soc.* **1993**, 115, 7685.

(21) (a) Bach, I.; Pörschke, K.-R.; Goddard, R.; Kopsike, C.; Krüger, C.; Rufinska, A.; Seevogel, M. *Organometallics* **1996**, 15, 4959. (b) Munakoto, M.; Ping Wu, L.; Kuroda-Sowa, T.; Maekawa, M.; Suenaga, Y.; Ling Ning, G.; Kojima, T. *J. Am. Chem. Soc.* **1998**, 120, 8610. (c) Cobbleddick, R. E.; Einstein, W. B. *Acta Crystallogr.* **1978**, B34, 1849. (d) Brauer, D. J.; Krüger, C. *Inorg. Chem.* **1977**, 16, 884. (e) Bell, T. W.; Helliwell, M.; Partridge, M. G.; Perutz, R. N. *Organometallics* **1992**, 11, 1911. (f) Müller, J.; Hirsch, C.; Qiao, K.; Ha, K. Z. *Anorg. Allg. Chem.* **1996**, 622, 1441. (g) van der Heijden, H.; Orpen, A. G.; Pasman, P. J. *J. Chem. Soc., Chem. Commun.* **1985**, 1576. (h) Winemiller, M. D.; Kelsch, B. A.; Sabat, M.; Harman, W. D. *Organometallics* **1997**, 16, 3672. (i) Scott, F.; Krüger, C.; Betz, P. *J. Organomet. Chem.* **1990**, 387, 113. (j) Stanger, A.; Boese, R. *J. Organomet. Chem.* **1992**, 430, 235. (k) Harman, W. D.; Gebhard, M.; Taube, H. *Inorg. Chem.* **1990**, 29, 567.

(22) Tagge, C. D.; Bergman, R. G. *J. Am. Chem. Soc.* **1996**, 118, 6908.

(23) Chin, R. M.; Dong, L.; Duckett, S. B.; Jones, W. D. *Organometallics* **1992**, 11, 871.

(24) Harman, W. D. *Chem. Rev.* **1997**, 97, 1953.

(25) Muetterties, E. L.; Bleeke, J. R.; Wucherer, E. J.; Albright, T. A. *Chem. Rev.* **1982**, 82, 499.

yielded the mononuclear and dinuclear  $\eta^2$ -naphthalene complexes, but the C–H activation product was not detected.<sup>20</sup>

To explore the qualitative and quantitative information concerning  $\eta^2$ -arene coordination that can be obtained by NOE spectroscopy, we have measured phase-sensitive <sup>1</sup>H–<sup>1</sup>H NOESY spectra of  $\eta^2$ -1,2-naphthalene and  $\eta^2$ -9,10-phenanthrene complexes of ( $\eta^5$ -cyclopentadienyl)(trimethylphosphine)rhodium. Polycyclic arenes are advantageous for this purpose, as they provide NOE interactions between nuclei of known internuclear separation that can be used for calibration to determine internuclear distances. Our spectra also revealed dynamic exchange processes in the naphthalene complex which we have studied by EXSY methods. We have determined the molecular structure of the dimer, [( $\eta^5$ -C<sub>5</sub>H<sub>5</sub>)Rh(PMe<sub>3</sub>)<sub>2</sub>( $\mu$ -1,2- $\eta^2$ -3,4- $\eta^2$ -C<sub>10</sub>H<sub>8</sub>)], crystallographically and compared the crystallographic data to averaged internuclear distances determined by NOESY for the mono- and dinuclear rhodium complexes.

### Experimental Section

All syntheses and manipulations were performed under nitrogen or argon using standard Schlenk (vacuum 10<sup>-2</sup> mbar) and high-vacuum (10<sup>-4</sup> mbar) techniques or in a glovebox. Chemicals were supplied by Aldrich and used as received. All solvents for general use were reagent grade or better and were dried by refluxing over sodium benzophenone and distilled under an inert atmosphere. Deuterated solvents were dried over potassium and distilled under vacuum prior to use. All NMR tubes were either fitted with concentric Young's stopcocks to allow sealing under an inert atmosphere or flame-sealed under vacuum. Samples were degassed prior to the acquisition with three freeze–pump–thaw cycles. Solutions for photolysis were prepared in small ampules fitted with ptfе stopcocks and were irradiated with an Applied Photophysics 250 W high-pressure mercury arc fitted with a water filter. Mass spectra were run on a VG Autospec.

**NMR Methods.** Spectra were recorded on a Bruker AMX500 spectrometer (<sup>1</sup>H spectra at 500.13 MHz, <sup>31</sup>P at 202.46 MHz, <sup>13</sup>C at 125.76 MHz). <sup>1</sup>H NMR chemical shifts were referenced to residual protiated solvent: *d*<sub>8</sub>-toluene ( $\delta$  2.10), *d*<sub>14</sub>-methylcyclohexane ( $\delta$  1.36), *d*<sub>12</sub>-cyclohexane ( $\delta$  1.38). <sup>31</sup>P{<sup>1</sup>H} NMR chemical shifts were referenced to external H<sub>3</sub>PO<sub>4</sub> (85%) at  $\delta$  0.0. <sup>13</sup>C{<sup>1</sup>H} NMR chemical shifts were referenced to solvent peaks: *d*<sub>8</sub>-toluene ( $\delta$  21.3).

*T*<sub>1</sub> values were measured by the standard inversion–recovery experiment with accurately calibrated ( $\pi$ )<sub>x</sub> and ( $\pi/2$ )<sub>x</sub> pulses (Bruker *t1ir1d* and *t1ir* pulse programs).<sup>1,2</sup> The recycle delay, *d*<sub>1</sub>, was set to 30 s. The results were analyzed using the 2D Bruker package, which fits the 1D peak integrals, *I*, to the expression  $I(t) = P + P^* \exp(-t/T_1)$ , where *P*\* is a constant.<sup>26</sup>

2D NOESY or EXSY spectra were recorded on a Bruker AMX500 spectrometer using the *noesytp* pulse program, which includes TPPI phase-cycling so as to generate phase-sensitive spectra.<sup>2,26</sup> The ( $\pi/2$ )<sub>x</sub> pulse length was calibrated before each experiment. The choice of mixing time  $\tau_m$  and recycle delay *d*<sub>1</sub> are discussed in the Results section. Spectra were typically acquired with 256 or 512 slices in the *F*<sub>1</sub> domain, and 4K or 6K points in *F*<sub>2</sub>. Spectra were processed with zero filling in the *F*<sub>1</sub> domain to double the number of slices. A sine window function was applied to the processed data. EXSY experiments were recorded at several values of  $\tau_m$  for each complex (all of around 20–30% of *T*<sub>1</sub>). An additional experiment was run with

**Table 1. Crystallographic Parameters and Structure Refinement for [( $\eta^5$ -C<sub>5</sub>H<sub>5</sub>)Rh(PMe<sub>3</sub>)<sub>2</sub>( $\eta^2$ -1,2- $\eta^2$ -3,4-C<sub>10</sub>H<sub>8</sub>)]**

empirical formula	C <sub>52</sub> H <sub>72</sub> P <sub>4</sub> Rh <sub>4</sub>
<i>M</i>	1232.62
color, dimens/mm	red, 0.40 × 0.38 × 0.36
cryst syst	monoclinic
space group	<i>P</i> 2 <sub>1</sub> / <i>c</i>
<i>a</i> /Å	11.120(9)
<i>b</i> /Å	15.739(5)
<i>c</i> /Å	30.07(2)
$\beta$ /deg	95.40(6)
<i>V</i> /Å <sup>3</sup>	5240(6)
<i>D</i> <sub>c</sub> /g cm <sup>-3</sup>	1.562 (calculated)
temperature/K	293(2)
Mo–K $\alpha$ radiation $\lambda$ /Å	0.71069
<i>Z</i>	4
abs coeff/mm <sup>-1</sup>	1.393
<i>F</i> (000)	2496
$\theta$ range/deg	2.54–25.02
index ranges	0 ≤ <i>h</i> ≤ 13, 0 ≤ <i>k</i> ≤ 18, –35 ≤ <i>l</i> ≤ 35
no. reflns measured, unique	9604, 9229 ( <i>R</i> <sub>int</sub> = 0.0324)
refinement method	full-matrix least-squares on <i>F</i> <sup>2</sup>
no. of data/restraints/params	9137/0/565
goodness-of-fit on <i>F</i> <sup>2</sup>	1.112
residuals [ <i>I</i> > 2 $\sigma$ ( <i>I</i> )]	<i>R</i> <sub>1</sub> = 0.0475, <i>wR</i> <sub>2</sub> = 0.1232
residuals (all data)	<i>R</i> <sub>1</sub> = 0.0781, <i>wR</i> <sub>2</sub> = 0.2248
largest diff peak and hole /e Å <sup>-3</sup>	0.796, –0.549

a mixing time,  $\tau_m$ , of 1 ms to allow *M*<sub>x</sub><sup>0</sup> values to be measured (see Analysis Section).<sup>10,13,14</sup>

**Crystallographic Methods.** X-ray data for [( $\eta^5$ -C<sub>5</sub>H<sub>5</sub>)Rh(PMe<sub>3</sub>)<sub>2</sub>( $\eta^2$ -1,2- $\eta^2$ -3,4-C<sub>10</sub>H<sub>8</sub>)] were collected on a Rigaku AFC6S diffractometer. Data reduction and Lorentz, polarization, and 2 $\theta$ -dependent corrections were applied with the TEXSAN system.<sup>27</sup> The structure was solved by direct methods by SHELXS86, with full-matrix least-squares refinement carried out with SHELXL93.<sup>28</sup> The hydrogen atoms were included at calculated sites and refined with a riding model except for H(1) to H(4), and H(27) to H(30), which were located in the final difference map. Their coordinates were refined independently, but their thermal parameters were set at 1.2 times those of the attached carbon atoms. Crystallographic data are listed in Table 1.

**Synthesis of ( $\eta^5$ -C<sub>5</sub>H<sub>5</sub>)Rh(PMe<sub>3</sub>)(C<sub>6</sub>H<sub>5</sub>)H.** ( $\eta^5$ -C<sub>5</sub>H<sub>5</sub>)Rh(PMe<sub>3</sub>)(C<sub>6</sub>H<sub>5</sub>) (53 mg, 2 × 10<sup>-4</sup> mol) was transferred to an ampule (5 cm<sup>3</sup> volume) under argon and dissolved in dry benzene (2.5 cm<sup>3</sup>).<sup>29</sup> The yellow solution was degassed (with three freeze–pump–thaw cycles) and put back under argon. The solution was photolyzed for 18–20 h ( $\lambda$  > 375 nm), during which time it darkened. The excess solvent was removed under vacuum to leave small white crystals. The extremely air-sensitive complex sublimed at ca. 315 K and 10<sup>-4</sup> mbar onto a liquid-nitrogen cooled finger and was stored in a glovebox prior to use. Yields in this reaction were poor.

**Synthesis of ( $\eta^5$ -C<sub>5</sub>H<sub>5</sub>)Rh(PMe<sub>3</sub>)( $\eta^2$ -C<sub>10</sub>H<sub>8</sub>).** ( $\eta^5$ -C<sub>5</sub>H<sub>5</sub>)Rh(PMe<sub>3</sub>)(C<sub>6</sub>H<sub>5</sub>)H, prepared as described above, was removed from the sublimation coldfinger in a glovebox. Naphthalene (~40 mg), dissolved in *d*<sub>14</sub>-methylcyclohexane, was then added and the mixture placed in an NMR tube and degassed.<sup>20</sup> The NMR tube was then heated for 7 h at 313 K, during which time the solution became a deep red color (prolonged heating, or the addition of less naphthalene, leads to formation of the dimer [( $\eta^5$ -C<sub>5</sub>H<sub>5</sub>)Rh(PMe<sub>3</sub>)<sub>2</sub>( $\mu$ -1,2- $\eta^2$ -3,4- $\eta^2$ -C<sub>10</sub>H<sub>8</sub>)]. The reaction can be followed by <sup>31</sup>P NMR: ( $\eta^5$ -C<sub>5</sub>H<sub>5</sub>)Rh(PMe<sub>3</sub>)(C<sub>6</sub>H<sub>5</sub>)H  $\delta$  15.17 (d, *J*<sub>RhP</sub> = 160.3 Hz); ( $\eta^5$ -C<sub>5</sub>H<sub>5</sub>)Rh(PMe<sub>3</sub>)( $\eta^2$ -C<sub>10</sub>H<sub>8</sub>)  $\delta$  3.76

(27) TEXSAN-TEXRAY Structure Analysis Package; Molecular Structure Corporation: The Woodlands, TX, 1985.

(28) Sheldrick, G. M. SHELXS 86. *Acta Crystallogr.* **1990**, *A46*, 467. Sheldrick, G. M. SHELXL 93, Program for the Refinement of Crystal Structures; University of Göttingen, 1995.

(29) Partridge, M. G. Ph.D. Thesis, University of York, 1992.

(26) Bruker Analytische, Messtechnik GmbH, 1989, 1990, 1991.

(d,  $J_{\text{RhP}} = 199.5$  Hz);  $[(\eta^5\text{-C}_5\text{H}_5)\text{Rh}(\text{PMe}_3)]_2(1,2\text{-}\eta^2\text{-3,4-}\eta^2\text{-C}_{10}\text{H}_8)$   $\delta$  5.05 (d,  $J_{\text{RhP}} = 207.6$  Hz). The solution was transferred to a Schlenk tube and the solvent removed under vacuum. Excess naphthalene was then removed by sublimation at 293–313 K and  $10^{-4}$  mbar, onto an iced-water-cooled finger. Attempts to remove all of the excess naphthalene led to decomposition or dimerization. The remaining dark red solid was dissolved in degassed  $d_{14}$ -methylcyclohexane, and the resulting solution was flame-sealed in an NMR tube under vacuum. In subsequent preparations, hexane was used as a solvent and the NMR tube replaced by an ampule.

A deep red crystal of  $[(\eta^5\text{-C}_5\text{H}_5)\text{Rh}(\text{PMe}_3)]_2(1,2\text{-}\eta^2\text{-3,4-}\eta^2\text{-C}_{10}\text{H}_8)$ , suitable for X-ray diffraction, was grown from  $d_{14}$ -methylcyclohexane in an NMR tube. The crystal was mounted in a Lindemann tube in a glovebox and sealed with epoxy cement.

MS (EI(+)):  $m/z$  488 ( $[(\eta^5\text{-C}_5\text{H}_5)\text{Rh}(\text{PMe}_3)]_2^+$ , 6%), 372 ( $[\text{M}]^+$ , 6%), 244 ( $[(\eta^5\text{-C}_5\text{H}_5)\text{Rh}(\text{PMe}_3)]^+$ , 91%), 168 ( $[\text{Rh}(\text{PMe}_3)]^+$ , 56%), 128 ( $[\text{C}_{10}\text{H}_8]^+$ , 100%), 76 ( $[\text{PMe}_3]^+$ , 26%). Accurate mass: measured 372.0524, calcd based on  $\text{C}_{18}\text{H}_{22}\text{PrH}$  372.0514, deviation 1.0 mDa.

**Synthesis of  $(\eta^5\text{-C}_5\text{H}_5)\text{Rh}(\text{PMe}_3)(9,10\text{-}\eta^2\text{-phenanthrene})$ .** The preparation followed the method used to prepare the  $\eta^5\text{-C}_5\text{Me}_5$  complex.<sup>18,20</sup>  $(\eta^5\text{-C}_5\text{H}_5)\text{Rh}(\text{PMe}_3)(\text{C}_6\text{H}_5)\text{H}$  (ca. 32 mg,  $1 \times 10^{-4}$  mol) was dissolved in  $d_{12}$ -cyclohexane, and excess (ca. 10 equiv) phenanthrene was added. The mixture was transferred to an NMR tube and heated to 323 K while following by NMR. The solution turned dark red on continued heating. The  $(\eta^5\text{-C}_5\text{H}_5)\text{Rh}(\text{PMe}_3)(\eta^2\text{-phenanthrene})$  was separated from the reaction mixture, which contained  $(\eta^5\text{-C}_5\text{H}_5)\text{Rh}(\text{PMe}_3)\text{-}(\text{Ph})\text{H}$ , free ligand, and traces of  $(\eta^5\text{-C}_5\text{H}_5)\text{Rh}(\text{PMe}_3)_2$  and  $(\eta^5\text{-C}_5\text{H}_5)\text{Rh}(\text{PMe}_3)(\text{C}_2\text{H}_4)$ , by recrystallization from  $d_{12}$ -cyclohexane. The resulting precipitate still contained some free phenanthrene.

In subsequent experiments, the reaction was performed on a larger scale in an ampule, with hexane as the solvent. The reaction was typically left for 2 days at 333 K. Much of the excess ligand was precipitated by cooling the sample to 243 K in a dry ice–acetone slush bath. The resulting red solution was decanted, concentrated, and left at approximately 243 K to crystallize. Large white crystals of phenanthrene and small red needles of  $(\eta^5\text{-C}_5\text{H}_5)\text{Rh}(\text{PMe}_3)(\eta^2\text{-C}_{14}\text{H}_{10})$  formed. The red needles were separated manually in a glovebox and dissolved in  $d_8$ -toluene to give an orange solution.  $^{13}\text{C}\{^1\text{H}\}$  NMR spectrum in  $d_8$ -toluene at 300 K:  $\delta$  (J/Hz) 20.4 (dd,  $J_{\text{PC}} = 27$ ,  $J_{\text{RhC}} = 1$ ,  $\text{PMe}_3$ ), 48.1 (dd,  $J_{\text{PC}} = 14$ ,  $J_{\text{RhC}} = 2$ ,  $\text{Rh-}\eta^2\text{-CH}$ ), 89.4 (dd,  $J_{\text{RhC}} = 3$ ,  $J_{\text{PC}} = 3$ ,  $\eta^5\text{-C}_5\text{H}_5$ ), 123.6 (s, CH), 124.8 (s, CH), 126.5 (s, CH), 129.4 (s, CH), 130.2 (s, C), 147.0 (s, C). The samples still contained some free phenanthrene, which prevented calculation of yields and reduced the relative intensity of the peaks due to complex in the mass spectra.

MS (EI(+)):  $m/z$  422 ( $[\text{M}]^+$ , 0.1%), 244 ( $[(\eta^5\text{-C}_5\text{H}_5)\text{Rh}(\text{PMe}_3)]^+$ , 0.5%), 179 ( $[\text{Rh}(\text{PMe}_3)]^+$ , 19%), 178 ( $[\text{C}_{14}\text{H}_{10}]^+$ , 100%).

## Analysis Section

For a first-order multispin system with a rigid conformation which undergoes chemical exchange and cross-relaxation, the peak intensities are given by<sup>30</sup>

$$\mathbf{I} = \mathbf{M}^0 \exp(-\mathbf{R}\tau_m) \quad (1)$$

where  $\mathbf{I}$  is the matrix of peak intensities (with elements  $I_{ix}$ , diagonal peak if  $i = x$ , cross-peak if  $i \neq x$ );  $\mathbf{M}^0$  is the matrix of equilibrium magnetizations of the nuclei (with

(30) The expression neglects cross-correlation terms, which is reasonable if the  $\tau_m$  used is less than the mixing time that gives maximum NOE cross-peak intensities.<sup>1,12</sup>

elements  $M_x^0$  corresponding to the intensity of the diagonal peak in site  $x$  when  $\tau_m = 0$ ); and  $\mathbf{R}$  is the relaxation matrix ( $N \times N$ ) that contains all the contributions to longitudinal relaxation.<sup>10,12–14</sup> The matrix  $\mathbf{R}$  has off-diagonal elements,  $R_{ix} = \sigma_{ix} - k_{ix}$ , and diagonal elements,  $R_{ii} = R_i + \sum_x k_{ix}$ , where  $\sigma_{ix}$  is the rate of cross-relaxation of nucleus  $i$  by nucleus  $x$ ,  $k_{ix}$  is the rate of chemical exchange between nuclei  $i$  and  $x$ , and  $R_{ii}$  is the total relaxation rate of nucleus  $i$ . Equation 1 can be solved exactly for a multispin system that shows NOE interactions and/or chemical exchange without making any assumptions about relaxation rates using the matrix method developed by Perrin and Gipe:<sup>12–14</sup>

$$\mathbf{R} = -\tau_m^{-1} \ln \mathbf{A} = -\tau_m^{-1} \mathbf{X}(\ln \Lambda)\mathbf{X}^{-1} \quad (2)$$

where  $\mathbf{A}$  has elements  $A_{ix} = I_{ix}/M_x^0$ ,  $\mathbf{X}$  is the matrix of eigenvectors of  $\mathbf{A}$ , such that  $\mathbf{X}^{-1}\mathbf{A}\mathbf{X} = \Lambda = \text{diag}(\lambda_i)$ ,  $\ln \Lambda = \text{diag}(\ln \lambda_i)$ , and  $\lambda_i$  is the  $i$ th eigenvalue of  $\mathbf{A}$  (all eigenvalues are positive). Values of  $M_x^0$  can be evaluated from a NOESY/EXSY experiment or from a matrix,  $\mathbf{P}$ , of the relative populations,  $p_b$ , of each site.<sup>14</sup> If the relative populations are used,  $k_{is}$  or  $\sigma_{is}$  can be determined, but the  $R_i$  values that contribute to the diagonal elements of  $\mathbf{R}$  cannot be found. The matrix method requires a complete set of peak intensities from all spins contributing to relaxation.

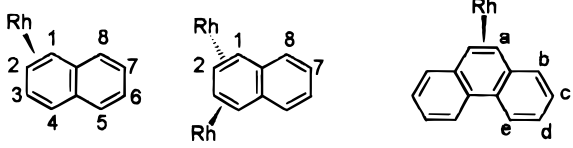
The method adopted for the NOESY spectra is illustrated below. From the peak integrals of the NOESY spectrum of  $(\eta^5\text{-C}_5\text{H}_5)\text{Rh}(\text{PMe}_3)(\eta^2\text{-C}_{10}\text{H}_8)$  at 260 K, the matrix of peak intensities,  $\mathbf{I}$ , was constructed for all protons except the cyclopentadienyl protons. Their omission is valid provided that they are not involved in the dipolar relaxation of the other protons. In this analysis,  $\mathbf{M}^0$  is replaced by  $\mathbf{P}$ , the matrix of relative populations,<sup>14</sup> viz., the diagonal matrix (9,1,1,1,1,1,1,1) which refers to the  $\text{PMe}_3$  protons and the naphthalene protons, H<sup>1</sup> to H<sup>8</sup>. The matrix  $\mathbf{A}$ , with elements given by  $I_{ij} \div M_j^0$ , was diagonalized to yield the matrices of its eigenvectors  $\mathbf{X}$  and its eigenvalues  $\Lambda$  and the relaxation matrix,  $\mathbf{R}$ , calculated according to eq 2 using Maple.<sup>31</sup> The off-diagonal elements of  $\mathbf{R}$  are equal to the rates of cross-relaxation between nucleus  $i$  and nucleus  $j$ ,  $\sigma_{ij}$ , assuming no exchange is occurring. Any values  $< 2 \times 10^{-3} \text{ s}^{-1}$  were assumed to be negligible.

The matrix analysis of the EXSY spectra was carried out as follows. From the peak integrals of  $(\eta^5\text{-C}_5\text{H}_5)\text{Rh}(\text{PMe}_3)(\eta^2\text{-C}_{10}\text{H}_8)$  at 300 K, the matrices of peak intensities,  $\mathbf{I}$ , were constructed for each of the mixing times used. In this analysis,  $\mathbf{M}^0$  was constructed using the diagonal peak intensities from an experiment with  $\tau_m$  of 1 ms.<sup>13</sup> The relaxation matrix,  $\mathbf{R}$ , was determined for each  $\tau_m$  value as above. The off-diagonal elements  $R_{ij}$  are equal to  $-k_{ji}$ , the rate of chemical exchange between nucleus  $j$  and nucleus  $i$ .

## Results

**1.  $^1\text{H}$ – $^1\text{H}$  NOESY Studies of  $(\eta^5\text{-C}_5\text{H}_5)\text{Rh}(\text{PMe}_3)(\eta^2\text{-C}_{10}\text{H}_8)$ .** When  $(\eta^5\text{-C}_5\text{H}_5)\text{Rh}(\text{PMe}_3)(\text{C}_6\text{H}_5)\text{H}$  is heated with excess naphthalene in hexane or  $d_{14}$ -methylcyclohexane, it is completely converted to the  $\eta^2$ -bound

(31) Maple V Release 4, Version 4.00b; Waterloo Maple Inc., 1996.

**Table 2.**  $^1\text{H}$  and  $^{31}\text{P}$  NMR Data [ $\delta$  (J/Hz)] Measured at 300 K for Complexes  $[\text{Rh}](\eta^2\text{-L})$  and  $[\text{Rh}]_2(\mu\text{-}\eta^2, \eta^2\text{-L})$ , Where  $[\text{Rh}] = (\eta^5\text{-C}_5\text{H}_5)\text{Rh}(\text{PMe}_3)$ 


complex/solvent	$^1\text{H}$ C <sub>5</sub> H <sub>5</sub>	$^1\text{H}$ PMe <sub>3</sub>	$^1\text{H}$ aromatic	$^{31}\text{P}$
$[\text{Rh}](\eta^2\text{-C}_{10}\text{H}_8)$ in $d_{14}$ -methylcyclohexane <sup>a</sup>	4.35 ( <i>ps</i> t, $J_{\text{RhH}} = J_{\text{PH}} = 0.7, 5$ H)	1.29 (dd, $J_{\text{PH}} = 9.3, J_{\text{RhH}} = 0.9, 9$ H)	3.49 (m, 1 H, H <sup>2</sup> ) 4.09 (td, 6.6, 2.6, 1 H, H <sup>1</sup> ) 6.42 (d, 8.8, 1 H, H <sup>4</sup> ) 7.05 (td, 7.6, 1.6, 1 H, H <sup>6</sup> ) 7.16 (m, 1 H, H <sup>3</sup> ) 7.17 (m, 1 H, H <sup>7</sup> ) 7.19 (m, 1 H, H <sup>5</sup> ) 7.63 (d, 7.6, 1 H)	3.76 (d, $J_{\text{RhP}} = 199.5$ )
$[\text{Rh}]_2(\mu\text{-}\eta^2, \eta^2\text{-C}_{10}\text{H}_8)$ in $d_{14}$ -methylcyclohexane <sup>a</sup>	4.55 ( <i>ps</i> t, $J_{\text{RhH}} = J_{\text{PH}} = 0.6, 10$ H)	1.29 (dd, $J_{\text{PH}} = 9.3, J_{\text{RhH}} = 0.9, 18$ H)	3.31 (m, 2 H, H <sup>1</sup> ) 3.91 (m, 2 H, H <sup>2</sup> ) 6.85 (dd, 5.7, 3.3, 2 H, H <sup>7</sup> ) 7.20 (dd, 5.7, 3.3, 2 H, H <sup>8</sup> )	5.05 (d, $J_{\text{RhP}} = 207.6$ )
$[\text{Rh}](\eta^2\text{-C}_{14}\text{H}_{10})$ in $d_8$ -toluene <sup>b-d</sup>	4.30 ( <i>ps</i> t, $J_{\text{RhH}} = J_{\text{PH}} = 0.65, 5$ H)	0.92 (dd, $J_{\text{PH}} = 9.1, J_{\text{RhH}} = 0.8, 9$ H)	3.93 (dd, 6.3, 2.7, 2 H, H <sup>a</sup> ) 7.14 (ddd, ~8, 8, 1.3, 2 H, H <sup>d</sup> ) 7.26 (ddd, ~8, 8, 1.1, 2 H, H <sup>c</sup> ) 7.72 (dd, ~8, 1.1, 2 H, H <sup>b</sup> ) 8.00 (d, ~8, 2 H, H <sup>e</sup> )	4.04 (d, $J_{\text{RhP}} = 197.7$ )

<sup>a</sup> Data ( $^1\text{H}$  300.13,  $^{31}\text{P}$  121.49 MHz) from refs 20, 29 with revised assignments based on  $^1\text{H}\{^{31}\text{P}\}$  NMR,  $^1\text{H}\text{-}^1\text{H}$  COSY, and  $^1\text{H}\text{-}^1\text{H}$  NOESY spectra and by comparison with refs 22 and 23. <sup>b</sup>  $^1\text{H}$  500.13,  $^{31}\text{P}$  202.46 MHz. Assignments based on 2D  $^1\text{H}\text{-}^1\text{H}$  NOESY and  $^1\text{H}\{^{31}\text{P}\}$  NMR spectra. <sup>c</sup> Free phenanthrene:  $^1\text{H}$  NMR data in  $d_8$ -toluene:  $\delta$  8.41 (d,  $J_{\text{HH}} \sim 8$  Hz, 2 H, H<sup>e</sup>), 7.63 (dd,  $J_{\text{HH}} \sim 8, 1.4$  Hz, 2 H, H<sup>b</sup>), 7.47 (s, 2 H, H<sup>a</sup>), 7.40 (ddd,  $J_{\text{HH}} \sim 8, 7, 1.5$  Hz, 2 H, H<sup>c</sup>), 7.36 (ddd,  $J_{\text{HH}} \sim 8, 7, 1.4$  Hz, 2 H, H<sup>d</sup>). <sup>d</sup>  $^1\text{H}$  NMR data for  $(\eta^5\text{-C}_5\text{H}_5)\text{Rh}(\text{PMe}_3)(\eta^2\text{-phenanthrene})$  in  $d_{12}$ -cyclohexane: 1.23 (dd, PMe<sub>3</sub>), 3.88 (dd, H<sup>a</sup>), 4.14 (dd,  $\eta^5\text{-C}_5\text{H}_5$ ), 7.06 (ddd, H<sup>d</sup>), 7.15 (ddd, H<sup>c</sup>), 7.54 (dd, H<sup>b</sup>), 7.95 (dd, H<sup>e</sup>).

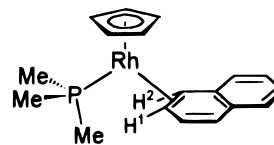
**Table 3.** Proton  $T_1$  Values/s for  $(\eta^5\text{-C}_5\text{H}_5)\text{Rh}(\text{PMe}_3)(\eta^2\text{-L})$  (L = polycyclic aromatic)<sup>a</sup>

L = C <sub>10</sub> H <sub>8</sub>								
temp/K	C <sub>5</sub> H <sub>5</sub>	PMe <sub>3</sub>	H <sup>1</sup>	H <sup>2</sup>	H <sup>4</sup>	H <sup>6</sup>	H <sup>3,5,7</sup>	H <sup>8</sup>
300	~17	3.3	4.3	4.6	4.7	~5.6	4.9–5.7	4.9
260	~10	1.6	1.7	1.9	2.2	3.1	2.6	2.4
L = C <sub>14</sub> H <sub>10</sub>								
temp/K	C <sub>5</sub> H <sub>5</sub>	PMe <sub>3</sub>	H <sup>a</sup>	H <sup>b</sup>	H <sup>c</sup>	H <sup>d</sup>	H <sup>e</sup>	
300	>13	3.0	3.4	4.5	5.6	<i>b</i>	2.5	

<sup>a</sup> Operating frequency 500.13 MHz, L = C<sub>10</sub>H<sub>8</sub> in  $d_{14}$ -methylcyclohexane, L = C<sub>14</sub>H<sub>10</sub> in  $d_8$ -toluene. <sup>b</sup> Not measured, resonance overlaps with free ligand.

naphthalene species,  $(\eta^5\text{-C}_5\text{H}_5)\text{Rh}(\text{PMe}_3)(\eta^2\text{-1,2-C}_{10}\text{H}_8)$ .<sup>20</sup> Removal of all of the excess naphthalene proves difficult because this drives the equilibrium toward the dinuclear complex, but full NMR data were obtained in the presence of some free naphthalene. The NMR data are close to those for the  $(\eta^5\text{-C}_5\text{Me}_5)$  analogue.<sup>19,23</sup> The  $^1\text{H}$  NMR assignments (Table 2) have been altered slightly from those given previously in the light of the NOESY spectra reported below.<sup>20</sup>

The spin–lattice relaxation times,  $T_1$ , for  $(\eta^5\text{-C}_5\text{H}_5)\text{Rh}(\text{PMe}_3)(\eta^2\text{-C}_{10}\text{H}_8)$  were measured in  $d_{14}$ -methylcyclohexane at 300 K (Table 3). The  $T_1$  values for the resonances in the naphthalene ligand lie between 4.3 and 5.7 s, but the value for the  $(\eta^5\text{-C}_5\text{H}_5)$  protons is much longer. The mixing time,  $\tau_m$ , was set to be ca. 20–30% of  $T_1$  for the naphthalene protons. The recycle delay,  $d_1$ , for a quantitative NOESY experiment should ideally be set to 3–5 times the longest  $T_1$  value, but a compromise value of 20 s was employed to allow a reasonable experiment time. Since there are no significant interactions involving the  $\eta^5\text{-C}_5\text{H}_5$  resonance, this

**Scheme 2.** Solution Structure for  $(\eta^5\text{-C}_5\text{H}_5)\text{Rh}(\text{PMe}_3)(\eta^2\text{-1,2-C}_{10}\text{H}_8)$  Proposed from NOESY Experiment

should give quantitative results for the other resonances.

The NOESY spectrum acquired at 300 K ( $\tau_m = 1.0$  s,  $d_1 = 20$  s,  $d_{14}$ -methylcyclohexane, Figure 2) shows cross-peaks arising from exchange (arrows) in addition to the NOE cross-peaks. The experiments were repeated at lower temperatures in order to reduce the rate of exchange. Lower temperatures had the further advantage of reducing the  $T_1$  values (Table 3) for the complex and the delays needed. The NOESY spectrum acquired at 260 K ( $d_1 = 15$  s,  $\tau_m$  1 s) showed NOE interactions (Table 4, column 1) and no exchange interactions.

The NOE cross-peaks which are significant in identifying the structure of  $(\eta^5\text{-C}_5\text{H}_5)\text{Rh}(\text{PMe}_3)(\eta^2\text{-1,2-C}_{10}\text{H}_8)$  are those between H<sup>1</sup> and the PMe<sub>3</sub> protons, and between H<sup>2</sup> and the PMe<sub>3</sub> protons. There are no NOE cross-peaks between the H<sup>1</sup> and H<sup>2</sup> protons and the  $\eta^5\text{-C}_5\text{H}_5$  ring. The NOE evidence shows that the hydrogens, H<sup>1</sup> and H<sup>2</sup>, attached to the  $\eta^2$ -bound carbon atoms of the naphthalene ring lie close in space to the PMe<sub>3</sub> methyl groups, suggesting a conformation with these hydrogens bent out of the plane of the naphthalene ring, away from the  $\eta^5\text{-C}_5\text{H}_5$  ring, and toward the PMe<sub>3</sub> group (Scheme 2). This structure agrees with all the known X-ray crystal structures for related complexes.<sup>18,21–23</sup>

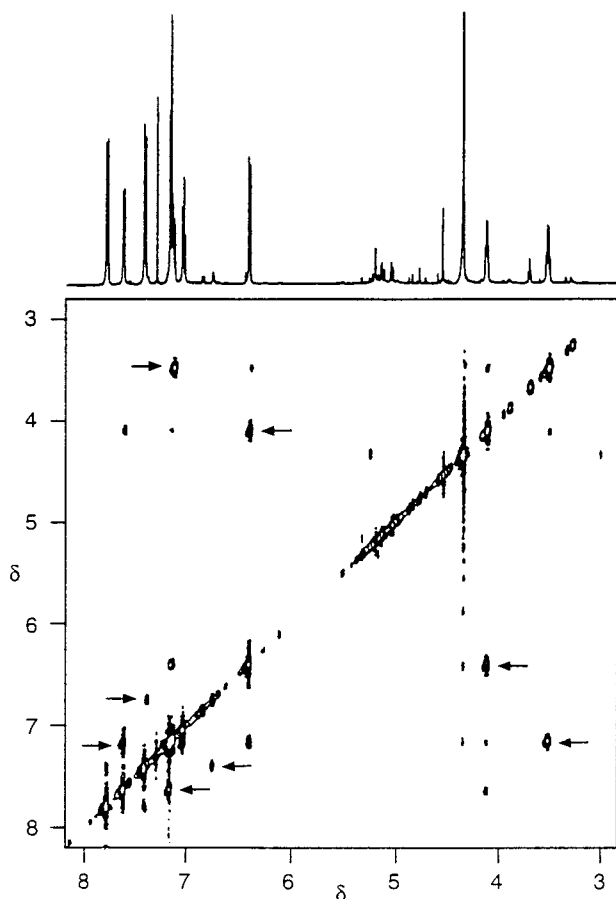


**Figure 2.** Section of the  $^1\text{H}$ - $^1\text{H}$  NOESY spectrum of  $(\eta^5\text{-C}_5\text{H}_5)\text{Rh}(\text{PMe}_3)(\eta^2\text{-C}_{10}\text{H}_8)$  in  $d_{14}$ -methylcyclohexane at 300 K (500.13 MHz,  $\tau_m = 1.0$  s,  $d_1 = 20$  s; exchange cross-peaks marked with arrows; other cross-peaks are negative and arise from NOE interactions).

Determination of internuclear distances requires integration of cross-peaks for protons at known separation as well as at unknown separation. The data collected at 260 K have short  $\tau_m$  values compared to the  $T_1$  values for the naphthalene hydrogens. The latter are close enough to one another in space to show NOE interactions. With  $(\eta^5\text{-C}_5\text{H}_5)\text{Rh}(\text{PMe}_3)(\eta^2\text{-C}_{10}\text{H}_8)$ , there is scalar coupling within each ring, but the spectrum does not show the distortions typical of a second-order system and  $J$ -cross-peaks make a negligible contribution to the NOE peak intensities.<sup>32</sup> The same applies to the other systems studied here.

NOE cross-peaks are seen between neighboring protons in the naphthalene ring, but no longer-range interactions can be detected. It is on this basis that the original NMR resonance assignments were altered (Table 2).<sup>20</sup> We tried the two-spin method of analysis based on the initial rate approximation, but found that

(32) If  $\Delta\nu > 20J$ , then the contribution to the cross-peak intensity from zero quantum coherence is below  $\pm 5\%$  and decreases as  $\Delta\nu$  increases ( $\Delta\nu$  = chemical shift difference between two nuclei  $i$  and  $s$  with scalar coupling constant  $J$ , both in Hz). For the majority of the cross-peaks for  $(\eta^5\text{-C}_5\text{H}_5)\text{Rh}(\text{PMe}_3)(\eta^2\text{-C}_{10}\text{H}_8)$  the minimum value of  $\Delta\nu/J$  is ca. 30. For the  $\text{H}^5$  to  $\text{H}^6$  and  $\text{H}^6$  and  $\text{H}^7$  interactions,  $\Delta\nu/J$  is less than 20, so the measured integrals for these NOE cross-peaks may be reduced (a less negative integral). The results from the EXSY experiments with different  $\tau_m$  values indicate that the contribution to the cross-peak intensities from zero quantum coherence is minimal. It is assumed that intramolecular dipolar relaxation is the only significant form of dipolar relaxation.

**Table 4.** NOE Cross Peak Intensities,  $I_{ij}$  and Matrix-Derived Cross-Relaxation Rates,  $\sigma_{ij}$  (arbitrary units) from NOESY Spectra for  $[\text{Rh}](\eta^2\text{-L})$  and  $[\text{Rh}]_2(\mu\text{-}\eta^2, \eta^2\text{-L})$ , Where  $[\text{Rh}] = (\eta^5\text{-C}_5\text{H}_5)\text{Rh}(\text{PMe}_3)$

complex, conditions	atoms	$I_{ij}$	$\sigma_{ij} \times 10^2$	relative $r_{\text{eff}}$
$[\text{Rh}](\eta^2\text{-C}_{10}\text{H}_8)$ $\tau_m = 1.0$ s, $d_1 = 15$ s $d_{14}$ -methylcyclohexane 260 K	$\text{PMe}_3 \leftrightarrow \text{H}^2$	12.54	0.38 <sup>b</sup>	1.53
	$\text{PMe}_3 \leftrightarrow \text{H}^1$	12.96	0.39 <sup>b</sup>	1.53
	$\text{H}^1 \leftrightarrow \text{H}^2$	12.71	3.5	1.06
	$\text{H}^2 \leftrightarrow \text{H}^3$	12.64	3.6	1.06
	$\text{H}^3 \leftrightarrow \text{H}^4$	16.74 <sup>a</sup>	5.0	1.00
	$\text{H}^4 \leftrightarrow \text{H}^5$	16.74 <sup>a</sup>	5.0	1.00
	$\text{H}^5 \leftrightarrow \text{H}^6$	11.71 <sup>a</sup>	3.7	1.05
	$\text{H}^6 \leftrightarrow \text{H}^7$	11.71 <sup>a</sup>	3.7	1.05
	$\text{H}^7 \leftrightarrow \text{H}^8$	13.42 <sup>a</sup>	4.5	1.02
$[\text{Rh}]_2(\mu\text{-}\eta^2, \eta^2\text{-C}_{10}\text{H}_8)$ $\tau_m = 1.0$ s, $d_1 = 15$ s $d_{14}$ -methylcyclohexane 260 K	$\text{PMe}_3 \leftrightarrow \text{H}^2$	2.82	0.37 <sup>b</sup>	1.57
	$\text{PMe}_3 \leftrightarrow \text{H}^1$	3.21	0.41 <sup>b</sup>	1.54
	$\text{H}^1 \leftrightarrow \text{H}^2$	3.20	5.5	1.00
	$\text{H}^1 \leftrightarrow \text{H}^8$	3.46	3.5	1.08
	$\text{H}^7 \leftrightarrow \text{H}^8$	2.88	2.9	1.11
$[\text{Rh}](\eta^2\text{-C}_{14}\text{H}_{10})$ $\tau_m = 1.2$ s, $d_1 = 20$ s $d_8$ -toluene at 300 K	$\text{PMe}_3 \leftrightarrow \text{H}^a$	2.194	0.46 <sup>b</sup>	1.37
	$\text{H}^a \leftrightarrow \text{H}^b$	2.199	3.1	1.00
	$\text{H}^b \leftrightarrow \text{H}^c$	1.973	2.7	1.03
	$\text{H}^c \leftrightarrow \text{H}^d$	1.620	1.9	1.08
	$\text{H}^d \leftrightarrow \text{H}^e$	2.157	3.1	1.00

<sup>a</sup> Measured cross-peak intensities between  $\text{H}^{3,5}$  and  $\text{H}^4$  and  $\text{H}^{5,7}$  and  $\text{H}^6$  were divided by 2 to take account of contributions from overlapping resonances. Matrix elements  $I_{ii}$  were approximated by dividing the total diagonal peak intensity for the overlapping  $\text{H}^3$ ,  $\text{H}^5$ , and  $\text{H}^7$  resonances by 3. <sup>b</sup>  $\sigma$  for a proton,  $\text{H}^a$ , relaxed by a  $\text{CH}_3$  group is equal to  $3 \times \sigma$  for the relaxation of the  $\text{CH}_3$  group by the proton,  $\text{H}^a$ .<sup>1b,6</sup> Thus,  $\sigma(\text{H} \text{ by } \text{PMe}_3) = 9 \times \sigma(\text{PMe}_3 \text{ by } \text{H})$ , and  $\sigma(\text{PMe}_3 \text{ by } \text{H}) \propto (r_{\text{eff}(\text{H} \leftrightarrow \text{PMe}_3)})^{-6}$ .

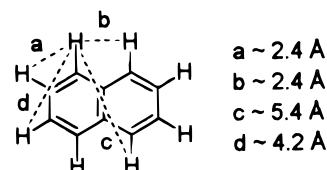


**Figure 3.** Approximate internuclear distances within the naphthalene ligand in  $(\eta^5\text{-C}_5\text{H}_5)\text{Rh}(\text{PMe}_3)(\eta^2\text{-C}_{10}\text{H}_8)$  based on  $r(\text{C}-\text{C})$  of 1.4 Å,  $r(\text{C}-\text{H})$  of 1.0 Å, and angles of  $120^\circ$ .

it gave unsatisfactory results.<sup>1,10,12</sup> On the other hand, the matrix method from Perrin and Gipe (see Analysis Section) worked well.<sup>13</sup> The raw cross-peak integrals,  $I_{ij}$ , are given in Table 4, column 2. The cross relaxation rates,  $\sigma_{ij}$ , determined by the matrix method and the corresponding relative effective internuclear distances,  $r_{\text{eff}}$ , are given in Table 4, columns 3 and 4. The internuclear distances are related to the cross-relaxation matrix elements,  $\sigma_{ij}$ , via the inverse sixth power,  $\sigma_{ij} \propto r_{\text{eff}}^{-6}$ .

We draw the following conclusions from these results.

(a) All the internuclear distances between nearest neighbor protons around the naphthalene ring are approximately equal (note that all values except those for  $\text{H}^1 \leftrightarrow \text{H}^2$  and  $\text{H}^1 \leftrightarrow \text{H}^8$  involve overlapping peaks). This conclusion agrees with the internuclear distances from the X-ray crystal structures of  $[(\eta^5\text{-C}_5\text{H}_5)\text{Rh}(\text{PMe}_3)]_2(\mu\text{-}\eta^2\text{-1,2-}\eta^2\text{-3,4-C}_{10}\text{H}_8)$  (see below) and free naphthalene,<sup>33</sup> which are nearly equal at 2.37 Å. Simple geometrical calculations (Figure 3) indicate that distances between non-neighboring hydrogens greatly exceed the limits for detectable NOE interactions.

(33) Brock, C. P.; Dunitz, J. D. *Acta Crystallogr., Sect. B* **1982**, *38*, 2218.

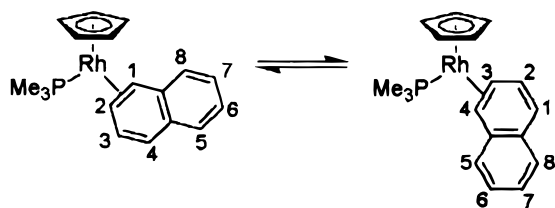
**Table 5. Mean Interatomic Distances (Å) between  $\text{PMe}_3$  Hydrogen Atoms and  $\text{H}^1$ ,  $\text{H}^2$  in Complexes of the Type  $[\text{Rh}](\eta^2\text{-L})$  and  $[\text{Rh}]_2(\mu\text{-}\eta^2, \eta^2\text{-L})$  ( $[\text{Rh}] = (\eta^5\text{-C}_5\text{H}_5)\text{Rh}(\text{PMe}_3)$ )**

complex	assumed H...H distance within ligand	$\text{PMe}_3 \leftrightarrow \text{H}^{2,1}$ distance from NOESY matrix method	$\text{PMe}_3 \leftrightarrow \text{H}^{2,1}$ distance from crystal structure <sup>a</sup>
$[\text{Rh}](\eta^2\text{-C}_{10}\text{H}_8)$	2.37	3.52	
$[\text{Rh}]_2(\mu\text{-}\eta^2, \eta^2\text{-C}_{10}\text{H}_8)$	2.37	3.48	3.56 <sup>b</sup>
$[\text{Rh}](\eta^2\text{-C}_{14}\text{H}_{10})$	see Figure 8	3.29	3.43 <sup>c</sup>

<sup>a</sup> Mean distances from crystal structure derived as in ref 41.

<sup>b</sup> Crystallographic data from this paper. <sup>c</sup> Crystallographic data for  $\eta^5\text{-C}_5\text{Me}_5$  complex from ref 19.

**Scheme 3. Exchange Process for  $(\eta^5\text{-C}_5\text{H}_5)\text{Rh}(\text{PMe}_3)(\eta^2\text{-C}_{10}\text{H}_8)$  at 300 K Identified Using EXSY Techniques**



(b) The NOESY spectrum indicates that the  $\text{H}^1$  and  $\text{H}^2$  are approximately equidistant from the averaged position of the  $\text{PMe}_3$  hydrogens and that this separation is larger than that between neighboring protons in the naphthalene ring. The rigid naphthalene ring system provides a series of suitable internuclear distances for calibration purposes. Thus, it is possible to use the known distance separating neighboring naphthalene protons (2.37 Å) and the relative  $r_{\text{eff}}$  values from Table 4, to estimate the mean effective internuclear distance between the hydrogens of the  $\eta^2$ -bound naphthalene and those of the phosphine methyl groups,  $r_{\text{eff}}$ , as 3.52 Å (Table 5). This calculation is in very good agreement with the separation of 3.56 Å calculated from the X-ray crystal structure of the dinuclear complex  $[(\eta^5\text{-C}_5\text{H}_5)\text{Rh}(\text{PMe}_3)]_2(\mu\text{-}\eta^2\text{-}1,2\text{-}\eta^2\text{-}3,4\text{-C}_{10}\text{H}_8)$  (see below).

**2. EXSY Study of Exchange in  $(\eta^5\text{-C}_5\text{H}_5)\text{Rh}(\text{PMe}_3)(\eta^2\text{-naphthalene})$ .** The phase-sensitive NOESY/EXSY spectra for  $(\eta^5\text{-C}_5\text{H}_5)\text{Rh}(\text{PMe}_3)(\eta^2\text{-C}_{10}\text{H}_8)$  acquired at 300 K (Figure 2) indicate that an exchange process occurs on the experimental time scale that converts  $\text{H}^1$  to  $\text{H}^4$ ,  $\text{H}^2$  to  $\text{H}^3$ ,  $\text{H}^5$  to  $\text{H}^8$ , and  $\text{H}^6$  to  $\text{H}^7$ . A consistent intramolecular exchange process (Scheme 3) involves hopping of the rhodium from one side of the ring to the other [C(1)–C(2) to C(3)–C(4)]. There is no evidence for the migration of the Rh center onto the noncoordinated naphthalene ring on this time scale. Intermolecular exchange with free naphthalene can be excluded, as cross-peaks cannot be seen between the resonances of the free and the coordinated naphthalene.

The EXSY spectra were recorded as a function of mixing time in order to determine the rate for the exchange process. EXSY spectra were recorded in  $d_{14}$ -methylcyclohexane at 300 K with  $d_1 = 20$  s and  $\tau_m$  values of 1 ms and 0.5, 1.0, and 1.5 s.<sup>34</sup> Since  $(\eta^5\text{-C}_5\text{H}_5)\text{Rh}(\text{PMe}_3)(\eta^2\text{-C}_{10}\text{H}_8)$  exists in equilibrium with a small

(34) The spectra suffered from  $F_2$  and  $F_1$  noise; the  $F_2$  noise was reduced by baseline correction, but the  $F_1$  ridge along the  $\text{PMe}_3$  and  $\eta^5\text{-C}_5\text{H}_5$  resonance positions was not completely removed. The artifacts do not affect the exchanging naphthalene resonances and so do not affect the analysis.

quantity of the C–H activation product  $(\eta^5\text{-C}_5\text{H}_5)\text{Rh}(\text{PMe}_3)(\text{C}_{10}\text{H}_7)\text{H}$  and the dimer (see below), all spectra were recorded at 300 K and the samples stored at room temperature between experiments in an attempt to keep this equilibrium steady and minimize its impact on the results of the EXSY analysis. Because of the overlap of the resonances for  $\text{H}^3$ ,  $\text{H}^5$ , and  $\text{H}^7$ , the integral of the diagonal peak for these resonances was divided by 3 to complete the matrices **I** and **M**<sup>0</sup>. The method of analyzing the EXSY spectra is described in the Analysis Section. The matrices of peak intensities, **I**, and relaxation rates, **R**, are both symmetrical, reflecting the equal populations of all of the sites involved in exchange.

The resulting pseudo-first-order rate constants,  $k_{xy}$ , for exchange of naphthalene protons in  $(\eta^5\text{-C}_5\text{H}_5)\text{Rh}(\text{PMe}_3)(\eta^2\text{-C}_{10}\text{H}_8)$  show little variation in the values of  $k_{xy}$  with  $\tau_m$ , which indicates that  $J$ -cross-peaks arising from scalar coupling make a negligible contribution to the intensities of the exchange cross-peaks.<sup>1,2,10</sup> The most reliable determinations of the rate constant should be those from measurement of  $k_{14}$  and  $k_{41}$ , which yield the pseudo-first-order rate constant at 300 K as  $(3.5 \pm 0.1) \times 10^{-1} \text{ s}^{-1}$ .<sup>35</sup> The other values ( $k_{23}$ ,  $k_{58}$ , and  $k_{67}$ ) suffer from inaccuracies caused by overlapping resonances and underlying NOE peaks and range from  $2.6 \times 10^{-1}$  to  $3.5 \times 10^{-1} \text{ s}^{-1}$ .

Green, Mann, and others have noted that the rate constants measured by dynamic NMR methods,  $k_{\text{obs}}$ , differ from those for the actual chemical exchange process,  $k_{\text{chem}}$ , and depend on the mechanism considered.<sup>36,37</sup> The difference arises because only those pathways for decay of the species at the midpoint of a symmetrical reaction profile that result in magnetization transfer will be observable by NMR techniques. For a certain proportion of the time, the chemical process will occur *without* observable magnetization transfer.<sup>37</sup> These problems are avoided by employing  $k_{\text{chem}}$ , which is calculated using the equation

$$k_{\text{chem}} = \alpha^{-1}[k_{\text{obs}}(\text{A} \rightarrow \text{B})]N_{\text{A}} \quad (3)$$

where  $\alpha = P_{\text{A}}P_{\text{B}}/(P_{\text{A}} + P_{\text{B}})$ ,  $P_{\text{A}}$  = number of nuclei in site A,  $P_{\text{B}}$  = number of nuclei in site B, and  $N_{\text{A}}$  = number of nuclei in site from which magnetization is transferred (here equal to  $P_{\text{A}}$ ).  $\Delta G^\ddagger$  is then given by the expression<sup>37</sup>

$$\Delta G^\ddagger = -RT \ln[k_{\text{chem}}h/k_{\text{B}}T] \quad (4)$$

where  $k_{\text{B}}$  is the Boltzmann constant,  $h$  is Planck's constant,  $R$  is the gas constant, and  $T$  is the temperature. In this system, the populations in the exchanging sites are equal,  $\alpha = 0.5$ , and  $N_{\text{A}} = 1$  (regardless of direction of reaction).<sup>37</sup> Thus,  $k_{\text{chem}} = 2k_{\text{obs}} = (7.0 \pm 0.1) \times 10^{-1} \text{ s}^{-1}$ . The free energy of activation for the exchange process,  $\Delta G^\ddagger_{300}$ , is 74.4 kJ mol<sup>-1</sup>.

**3. Equilibrium between  $(\eta^5\text{-C}_5\text{H}_5)\text{Rh}(\text{PMe}_3)(\eta^2\text{-}1,2\text{-C}_{10}\text{H}_8)$  and  $(\eta^5\text{-C}_5\text{H}_5)\text{Rh}(\text{PMe}_3)(\text{C}_{10}\text{H}_7)\text{H}$ .** The <sup>1</sup>H NMR spectrum of  $(\eta^5\text{-C}_5\text{H}_5)\text{Rh}(\text{PMe}_3)(\eta^2\text{-C}_{10}\text{H}_8)$  in  $d_{14}$ -

(35) The errors quoted here as the 95% confidence limits simply reflect the fact that the rate constants quoted are averaged. A full error analysis has not been attempted.

(36) Green, M. L. H.; Wong, L.-L.; Sella, A. *Organometallics* **1992**, *11*, 2660.

(37) Mann, B. E. *J. Chem. Soc., Perkin Trans. 2* **1977**, 84.

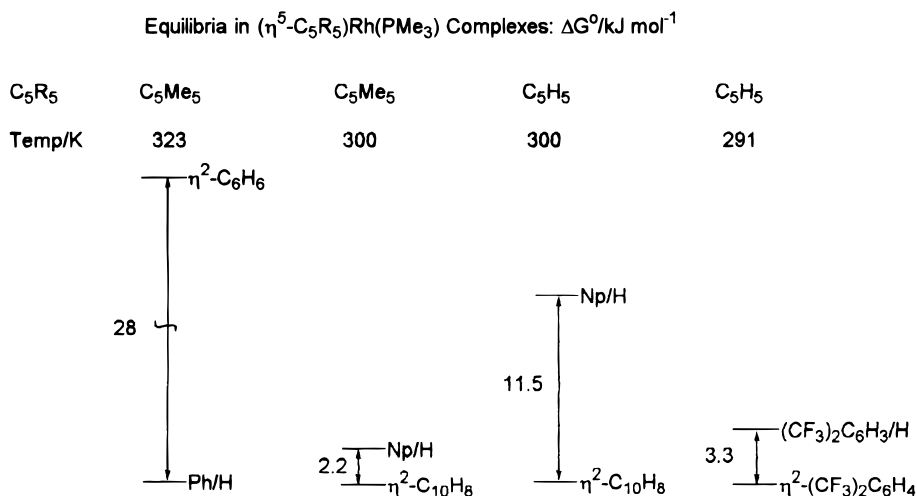


**Figure 4.** Relative free energy diagram for the interaction of the ( $\eta^5$ -C<sub>5</sub>H<sub>5</sub>)Rh(PMe<sub>3</sub>) and ( $\eta^5$ -C<sub>5</sub>Me<sub>5</sub>)Rh(PMe<sub>3</sub>) fragments with benzene, naphthalene, and 1,4-bis(trifluoromethyl)benzene. Note different temperatures for the different sets.<sup>18,20</sup> In each case, the lower state is shown as the free energy zero.

methylcyclohexane at 300 K provides evidence of an additional hydride-containing species ( $\delta$  -13.84, dd,  $J_{\text{PH}} = 43.2$  Hz,  $J_{\text{RhH}} = 30.5$  Hz). The corresponding <sup>31</sup>P NMR resonance is detected as a very weak doublet at  $\delta$  15.15 ( $J_{\text{RHP}} = 160.4$  Hz). It therefore appears that ( $\eta^5$ -C<sub>5</sub>H<sub>5</sub>)Rh(PMe<sub>3</sub>)( $\eta^2$ -C<sub>10</sub>H<sub>8</sub>) may exist in equilibrium with a naphthyl-hydride isomer as was observed in the  $\eta^5$ -C<sub>5</sub>Me<sub>5</sub> case.<sup>19,20</sup> By analogy with the latter system, it is probable that the 2-naphthyl isomer is formed (Scheme 1). The hydride and phosphorus NMR resonances for ( $\eta^5$ -C<sub>5</sub>H<sub>5</sub>)Rh(PMe<sub>3</sub>)(C<sub>6</sub>H<sub>5</sub>)H and ( $\eta^5$ -C<sub>5</sub>H<sub>5</sub>)Rh(PMe<sub>3</sub>)(2-naphthyl)H are very similar,<sup>18,19</sup> just as is the case for the  $\eta^5$ -C<sub>5</sub>Me<sub>5</sub> analogues.

To determine the ratio of the two isomers in the  $\eta^5$ -C<sub>5</sub>H<sub>5</sub> case, quantitative <sup>31</sup>P NMR spectra were acquired at 300 K in *d*<sub>14</sub>-methylcyclohexane (202.46 MHz with over 2000 scans, recycle delay 20 s, chosen on the basis of the <sup>31</sup>P NMR *T*<sub>1</sub> value of C<sub>5</sub>Me<sub>5</sub> complexes).<sup>20</sup> The isomer ratio was determined to be approximately 100:1 for the  $\eta^2$ -naphthalene and the naphthyl-hydride complexes (cf. 2:1 ratio at 333 K for the C<sub>5</sub>Me<sub>5</sub> analogues).<sup>19</sup>

The observation that ( $\eta^5$ -C<sub>5</sub>H<sub>5</sub>)Rh(PMe<sub>3</sub>)( $\eta^2$ -C<sub>10</sub>H<sub>8</sub>) exists in equilibrium with a small amount of the C-H activation product is consistent with the earlier work,<sup>18,20</sup> which demonstrated that such equilibria can be controlled by changes in the ligation. Thus, the  $\eta^5$ -C<sub>5</sub>Me<sub>5</sub> ligand tends to push the equilibrium between the Rh<sup>I</sup>  $\eta^2$ -arene species and the Rh<sup>III</sup> aryl-hydride toward the Rh<sup>III</sup> species. For the ( $\eta^5$ -C<sub>5</sub>Me<sub>5</sub>) equilibrium, the free energy change for the conversion from  $\eta^2$ -naphthalene to (naphthyl)hydride complex,  $\Delta G^\circ_{300}$ , is +2.2 kJ mol<sup>-1</sup>, while for the ( $\eta^5$ -C<sub>5</sub>H<sub>5</sub>) equilibrium,  $\Delta G^\circ_{300}$  is +11.5 kJ mol<sup>-1</sup>. The difference in free energy difference,  $\Delta\Delta G^\circ_{300}$  is -9.3 kJ mol<sup>-1</sup> (defined as  $\{\Delta G^\circ_{300}(\eta^5\text{-C}_5\text{Me}_5) - \Delta G^\circ_{300}(\eta^5\text{-C}_5\text{H}_5)\}$ , Figure 4).<sup>18,20</sup>

**4. Molecular Structure of [( $\eta^5$ -C<sub>5</sub>H<sub>5</sub>)Rh(PMe<sub>3</sub>)]<sub>2</sub>( $\mu$ -1,2- $\eta^2$ -3,4- $\eta^2$ -C<sub>10</sub>H<sub>8</sub>).** The thermal reaction of naphthalene with ( $\eta^5$ -C<sub>5</sub>H<sub>5</sub>)Rh(PMe<sub>3</sub>)(C<sub>6</sub>H<sub>5</sub>)H leads to the formation of the dimeric species [( $\eta^5$ -C<sub>5</sub>H<sub>5</sub>)Rh(PMe<sub>3</sub>)]<sub>2</sub>(1,2- $\eta^2$ -3,4- $\eta^2$ -C<sub>10</sub>H<sub>8</sub>) in addition to ( $\eta^5$ -C<sub>5</sub>H<sub>5</sub>)Rh(PMe<sub>3</sub>)( $\eta^2$ -C<sub>10</sub>H<sub>8</sub>) on prolonged heating or the removal of the excess naphthalene (NMR data in Table 2).<sup>20</sup>

Jones et al.<sup>23</sup> investigated the analogous  $\eta^5$ -C<sub>5</sub>Me<sub>5</sub> system, while Harman and Taube studied [(M(NH<sub>3</sub>)<sub>5</sub>)<sub>2</sub>-

( $\mu$ - $\eta^2$ : $\eta^2$ -C<sub>10</sub>H<sub>8</sub>)](OTf)<sub>4</sub> (M = Os, Os; Os, Ru).<sup>24,38,39</sup> They showed that the dinuclear and the mononuclear systems exist in equilibrium and that the monomer is the kinetic product while the dimer is the thermodynamic product. On heating, ( $\eta^5$ -C<sub>5</sub>Me<sub>5</sub>)Ru(NO)( $\eta^2$ -1,2-C<sub>10</sub>H<sub>8</sub>) dimerizes in an analogous manner,<sup>22</sup> and a similar dimer is formed directly by reaction of TpRe(CO)<sub>2</sub>(THF) (Tp = hydridotris(pyrazolyl)borate) with naphthalene.<sup>40</sup> In our system, the dimer was formed if the excess naphthalene was removed from a sample of ( $\eta^5$ -C<sub>5</sub>H<sub>5</sub>)Rh(PMe<sub>3</sub>)( $\eta^2$ -C<sub>10</sub>H<sub>8</sub>) and the solution left at low temperature, providing evidence for an analogous equilibrium (Scheme 1). This observation explains the difficulties in isolating and crystallizing the monomer.

A deep red crystal of the [( $\eta^5$ -C<sub>5</sub>H<sub>5</sub>)Rh(PMe<sub>3</sub>)]<sub>2</sub>( $\mu$ -1,2- $\eta^2$ -3,4- $\eta^2$ -C<sub>10</sub>H<sub>8</sub>) dimer suitable for X-ray analysis was grown from *d*<sub>14</sub>-methylcyclohexane. The X-ray crystal structure (Figure 5) is very similar to that of the  $\eta^5$ -C<sub>5</sub>Me<sub>5</sub> analogue prepared by Jones et al. but of higher quality.<sup>23</sup> As in the  $\eta^5$ -C<sub>5</sub>Me<sub>5</sub> case, there are two independent molecules within the asymmetric unit, **A** and **B**.<sup>23</sup> The hydrogen atoms H(1), H(2), H(3), and H(4) were located in the final Fourier difference map. Selected bond lengths and angles for both molecules **A** and **B** are given in Table 6.

In agreement with structures mentioned above,<sup>21,23–25</sup> the metal fragments coordinate to opposite faces of the naphthalene ring, keeping the rhodium atoms 5.01 Å from one another. The C-C bond lengths in the coordinated naphthalene ring are compared to free naphthalene in Figure 6.<sup>33</sup> All of the C-C bonds of the coordinated ring are lengthened relative to the free ligand, and there is conspicuous bond length alternation, consistent with the loss of aromatic character. In contrast, the distortions of the noncoordinated ring render this ring more "aromatic" in character than in the free ligand, which exhibits a C-C/C=C bonding pattern around the ring. The NMR data show that the

(38) Harman, W. D.; Taube, H. *J. Am. Chem. Soc.* **1988**, *110*, 7555.

(39) (a) Harman, W. D.; Taube, H. *J. Am. Chem. Soc.* **1987**, *109*, 1883. (b) Harman, W. D.; Sekine, M.; Taube, H. *J. Am. Chem. Soc.* **1988**, *110*, 5725.

(40) Gunnoe, T. B.; Sabat, M.; Harman, W. D. *J. Am. Chem. Soc.* **1998**, *120*, 8747.

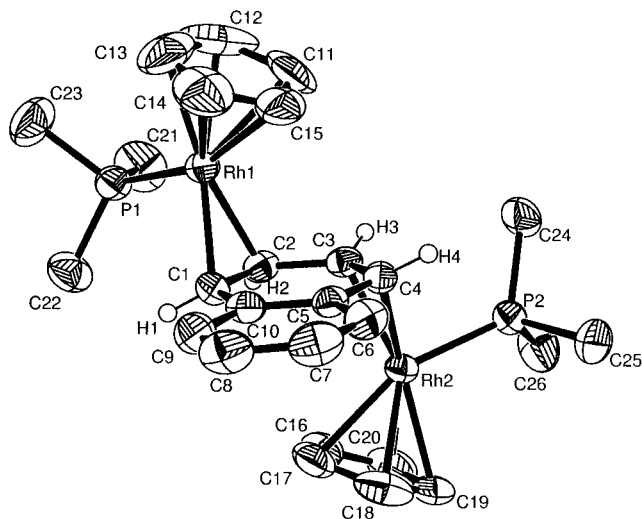


**Figure 5.** X-ray crystal structure of  $[(\eta^5\text{-C}_5\text{H}_5)\text{Rh}(\text{PMe}_3)]_2 \cdot (\mu\text{-}1,2\text{-}\eta^2\text{-}3,4\text{-}\eta^2\text{-C}_{10}\text{H}_8)$ . The probability ellipsoids are shown at the 50% level. Hydrogen atoms are omitted except for those bound to the carbon atoms coordinated to rhodium. Only molecule **A** is shown.

resonances corresponding to the uncoordinated naphthalene ring closely resemble the resonances for free naphthalene ( $\delta$  7.4 and 7.8,  $[\text{AX}]_2$  system).

The rhodium atoms Rh(1) to Rh(4) lie between 2.010 and 2.021 Å from the midpoint (D(2)) of the  $\eta^2\text{-C}=\text{C}$  bond. The carbon atoms of the naphthalene rings are almost coplanar (rms deviation of 0.016 Å for molecule **A** and 0.046 Å for molecule **B**). For molecule **A**, the angles between the naphthalene ring and the cyclopentadienyl rings are 27.8(3)° and 24.2(3)°. For molecule **B**, the corresponding angles are 29.1(4)° and 28.0(4)°. The  $\eta^2$ -coordination is symmetric, with the Rh–C bond distances differing by a maximum of 0.017 Å. The hydrogen atoms on the  $\eta^2$ -bound carbon atoms [H(1) to H(4) and H(27) to H(30)] show the characteristic distortion out of the plane of the naphthalene ligand, away from the  $\eta^5\text{-C}_5\text{H}_5$  ring. For molecule **A**, the angle between the plane defined by C(1)C(2)H(1)H(2) and the naphthalene plane is 32(6)° and that between the naphthalene plane and plane C(3)C(4)H(3)H(4) is 24(5)°. For molecule **B**, the corresponding values are 34(3)° and 24(5)°. These parameters compare favorably with those for other  $\eta^2$ -naphthalene complexes (Figure 1).<sup>21–23</sup> The effective through-space distances from each  $\eta^2$ -bound proton to the nine appropriate methyl protons were averaged as  $1/\langle r^{-3} \rangle^{1/3}$  (see Introduction).<sup>7</sup> Since each molecule contains four  $\eta^2$ -bound protons and there are two independent molecules within the unit cell, a total of eight such effective distances are obtained. The arithmetic mean of these eight determinations yields a mean separation of 3.56 Å, which may be compared to the NOESY data (Table 5).<sup>41</sup>

**5. Structural Characterization of  $[(\eta^5\text{-C}_5\text{H}_5)\text{Rh}(\text{PMe}_3)]_2(\eta\text{-}1,2\text{-}\eta^2\text{-}3,4\text{-}\mu^2\text{-C}_{10}\text{H}_8)$  by NOESY.** The  $^1\text{H}$ – $^1\text{H}$  NOESY spectrum of the dimer was recorded at 260 K ( $\tau_m = 1.0$  s, recycle delay of 15 s). The  $T_1$  values for the dimer at this temperature are about 2.2–2.9 s for the hydrogens on the noncoordinated naphthalene ring, about 1.4–2.2 s for the hydrogens on the  $\eta^2$ -bound carbons, and about 9 s for the  $\eta^5\text{-C}_5\text{H}_5$  ligands. The main NOE cross-peaks observed for the dimer are given in

**Table 6.** Selected Bond Lengths and Angles for  $[(\eta^5\text{-C}_5\text{H}_5)\text{Rh}(\text{PMe}_3)]_2(\mu\text{-}\eta^2\text{-}1,2\text{-}\eta^2\text{-}3,4\text{-C}_{10}\text{H}_8)$  with Estimated Standard Deviations in Parentheses

Molecule A		Molecule B	
bond	length/Å	bond	length/Å
Rh(1)–C(1)	2.146(8)	Rh(4)–C(29)	2.145(8)
Rh(1)–C(2)	2.138(8)	Rh(4)–C(30)	2.128(8)
Rh(1)–P(1)	2.209(3)	Rh(4)–P(4)	2.214(3)
Rh(1)–C(11)	2.277(10)	Rh(4)–C(42)	2.249(9)
Rh(2)–C(3)	2.145(8)	Rh(3)–C(27)	2.130(8)
Rh(2)–C(4)	2.129(8)	Rh(3)–C(28)	2.136(9)
Rh(2)–P(2)	2.217(3)	Rh(3)–P(3)	2.225(2)
Rh(2)–C(16)	2.292(10)	Rh(3)–C(37)	2.265(10)
C(1)–C(2)	1.419(12)	C(27)–C(28)	1.425(12)
C(1)–C(10)	1.462(12)	C(27)–C(36)	1.461(12)
C(2)–C(3)	1.485(11)	C(28)–C(29)	1.481(12)
C(3)–C(4)	1.426(11)	C(29)–C(30)	1.433(11)
C(4)–C(5)	1.469(11)	C(30)–C(31)	1.458(11)
C(5)–C(6)	1.403(11)	C(31)–C(32)	1.402(12)
C(6)–C(7)	1.387(13)	C(32)–C(33)	1.376(13)
C(7)–C(8)	1.392(14)	C(33)–C(34)	1.38(2)
C(8)–C(9)	1.386(13)	C(34)–C(35)	1.382(15)
C(9)–C(10)	1.378(12)	C(35)–C(36)	1.406(12)
C(5)–C(10)	1.407(11)	C(31)–C(36)	1.407(11)
C(1)–H(1)	0.89(9)	C(27)–H(27)	0.95(9)
C(2)–H(2)	0.89(9)	C(28)–H(28)	0.92(9)
C(3)–H(3)	0.99(8)	C(29)–H(29)	1.02(8)
C(4)–H(4)	0.93(9)	C(30)–H(30)	1.01(9)

Molecule A			
bond	angle/deg	bond	angle/deg
C(2)–Rh(1)–C(1)	38.7(3)	C(4)–Rh(2)–C(3)	39.0(3)
C(2)–Rh(1)–P(1)	93.0(2)	C(4)–Rh(2)–P(2)	90.9(2)
C(1)–Rh(1)–P(1)	94.4(2)	C(3)–Rh(2)–P(2)	94.2(2)
C(24)–P(2)–Rh(2)	121.7(3)	C(10)–C(1)–Rh(1)	112.3(5)
C(25)–P(2)–Rh(2)	114.7(4)	C(3)–C(4)–Rh(2)	71.1(4)
C(26)–P(2)–Rh(2)	114.5(4)	C(5)–C(4)–Rh(2)	112.8(5)
C(21)–P(1)–Rh(1)	116.3(4)	C(4)–C(3)–Rh(2)	69.9(4)
C(22)–P(1)–Rh(1)	119.8(4)	C(2)–C(3)–Rh(2)	114.8(5)
C(23)–P(1)–Rh(1)	115.8(4)	C(1)–C(2)–Rh(1)	71.0(5)
C(2)–C(1)–C(10)	120.5(8)	C(3)–C(2)–Rh(1)	112.4(5)
C(2)–C(1)–Rh(1)	70.4(5)		
Molecule B			
bond	angle/deg	bond	angle/deg
C(30)–Rh(4)–C(29)	39.2(3)	C(27)–Rh(3)–C(28)	39.0(3)
C(30)–Rh(4)–P(4)	92.5(2)	C(27)–Rh(3)–P(3)	92.4(2)
C(29)–Rh(4)–P(4)	94.2(2)	C(28)–Rh(3)–P(3)	93.1(2)
C(48)–P(3)–Rh(3)	120.5(4)	C(29)–C(30)–Rh(4)	113.4(5)
C(49)–P(3)–Rh(3)	115.5(4)	C(31)–C(30)–Rh(4)	69.8(4)
C(47)–P(3)–Rh(3)	115.5(4)	C(30)–C(29)–Rh(4)	113.0(6)
C(51)–P(4)–Rh(4)	113.0(4)	C(28)–C(29)–Rh(4)	70.3(5)
C(52)–P(4)–Rh(4)	121.9(3)	C(27)–C(28)–Rh(3)	115.8(6)
C(50)–P(4)–Rh(4)	70.7(5)	C(29)–C(28)–Rh(3)	116.3(4)
C(28)–C(27)–Rh(3)	113.2(5)	C(36)–C(27)–Rh(3)	71.1(5)

Table 4; additional small cross-peaks were observed from H<sup>1</sup>, H<sup>2</sup>, and PMe<sub>3</sub> to C<sub>5</sub>H<sub>5</sub>. There are large NOE interactions between the hydrogens bound to the  $\eta^2$ -coordinated carbons and the PMe<sub>3</sub> methyls, as expected from the solid-state structure.

The matrix analysis follows the same pattern as above (Table 4). It should be noted that signal overlap made measurement of the peak intensities for the on-diagonal

(41) The effective internuclear distance between each of the  $\eta^2$ -bound hydrogens and the phosphine methyls was calculated as follows. For each of the  $\eta^2$ -bound hydrogens, nine sets of static distances,  $r$ , to each of the methyl hydrogens of the PMe<sub>3</sub> ligand were measured from the X-ray crystal structure. The nine distances were averaged according to  $1/\langle r^{-3} \rangle^{1/3}$  to generate one effective distance from each of the  $\eta^2$ -bound hydrogens to the phosphine hydrogens. From the two independent molecules within the asymmetric unit, eight such effective internuclear separations were determined: H(1) ↔ PMe<sub>3</sub> averages 3.55 Å; H(2) ↔ PMe<sub>3</sub> 3.75 Å; H(3) ↔ PMe<sub>3</sub> 3.57 Å; H(4) ↔ PMe<sub>3</sub> 3.49 Å; H(27) ↔ PMe<sub>3</sub> 3.55 Å; H(28) ↔ PMe<sub>3</sub> 3.50 Å; H(29) ↔ PMe<sub>3</sub> 3.53 Å; H(30) ↔ PMe<sub>3</sub> 3.56 Å. The average of these eight distances is 3.56 Å.

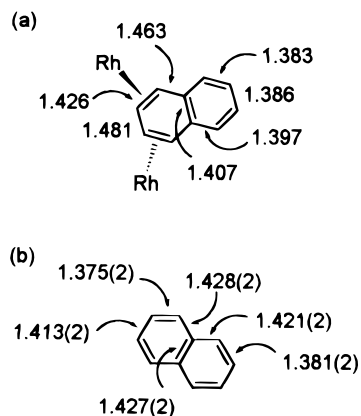


**Figure 6.** (a) C–C bond lengths (Å) in the naphthalene ligand in molecule **A** of  $[(\eta^5\text{-C}_5\text{H}_5)\text{Rh}(\text{PMe}_3)]_2(\mu\text{-}1,2\text{-}\eta^2\text{-}3,4\text{-}\eta^2\text{-C}_{10}\text{H}_8)$ . (b) C–C bond lengths (Å) for free naphthalene from an X-ray crystal structure determined at 184 K.<sup>33</sup>

peaks problematic. NOE interactions are seen between nearest neighbor protons around the naphthalene ring, and all the corresponding internuclear distances are approximately equal. Using the known distance separating neighboring naphthalene protons (2.37 Å) and the average of relative  $r_{\text{eff}}$  values listed in Table 4, we estimate  $r_{\text{eff}}$  as 3.48 Å, in good agreement with the separation of 3.56 Å calculated from the X-ray crystal structure (Table 5).

**6. NMR Study of  $(\eta^5\text{-C}_5\text{H}_5)\text{Rh}(\text{PMe}_3)(9,10\text{-}\eta^2\text{-phenanthrene})$ .** In addition to their work with  $(\eta^5\text{-C}_5\text{Me}_5)\text{Rh}(\text{PMe}_3)(\eta^2\text{-C}_{10}\text{H}_8)$ , Jones and Dong reported the synthesis and crystal structure of the related  $(\eta^5\text{-C}_5\text{Me}_5)\text{Rh}(\text{PMe}_3)(9,10\text{-}\eta^2\text{-phenanthrene})$  complex.<sup>19</sup> As for  $[(\eta^5\text{-C}_5\text{Me}_5)\text{Rh}(\text{PMe}_3)]_2(\mu\text{-}1,2\text{-}\eta^2\text{-}3,4\text{-}\eta^2\text{-C}_{10}\text{H}_8)$ ,<sup>23</sup> the crystal structure of the phenanthrene complex shows that the hydrogen atoms attached to the  $\eta^2$ -bound carbons are bent out of the plane of the arene ring and away from the  $\eta^5\text{-C}_5\text{Me}_5$  ligand.<sup>42</sup> Müller et al. reported a very similar structure for  $(\eta^5\text{-C}_5\text{H}_5)\text{Rh}(\text{C}_2\text{H}_4)(9,10\text{-}\eta^2\text{-phenanthrene})$ .<sup>21f</sup> To overcome the problem of  $^1\text{H}$  NMR signal overlap encountered for  $(\eta^5\text{-C}_5\text{H}_5)\text{Rh}(\text{PMe}_3)(\eta^2\text{-C}_{10}\text{H}_8)$  in analysis of the NOESY data and avoid dimer formation, we investigated  $(\eta^5\text{-C}_5\text{H}_5)\text{Rh}(\text{PMe}_3)(\eta^2\text{-phenanthrene})$ .

The thermal reaction of  $(\eta^5\text{-C}_5\text{H}_5)\text{Rh}(\text{PMe}_3)(\text{C}_6\text{H}_5)\text{H}$  with an excess of phenanthrene produced a single new complex (cf. the synthesis of the  $\eta^5\text{-C}_5\text{Me}_5$  analogue).<sup>18–20</sup> The product is assigned as  $(\eta^5\text{-C}_5\text{H}_5)\text{Rh}(\text{PMe}_3)(9,10\text{-}\eta^2\text{-phenanthrene})$  from the NMR data (Table 2) and by comparison with those for the  $\eta^5\text{-C}_5\text{Me}_5$  analogue and  $(\eta^5\text{-C}_5\text{Me}_5)\text{Ru}(\text{NO})(9,10\text{-}\eta^2\text{-phenanthrene})$ .<sup>19,20,22</sup> The  $^{31}\text{P}$  NMR spectrum shows the upfield shift and increase in coupling constant that is typical of a change from Rh(III) to Rh(I).<sup>18</sup>

The signal overlap problems that limited the use of the NOESY data for  $(\eta^5\text{-C}_5\text{H}_5)\text{Rh}(\text{PMe}_3)(\eta^2\text{-C}_{10}\text{H}_8)$  are much reduced. Accordingly,  $T_1$  data were collected (Table 3) and a  $^1\text{H}$ – $^1\text{H}$  NOESY spectrum of  $(\eta^5\text{-C}_5\text{H}_5)\text{Rh}(\text{PMe}_3)(9,10\text{-}\eta^2\text{-phenanthrene})$  was recorded with recycle delay of 4 s and  $\tau_m$  of 1.6 s (Figure 7). A further

(42) The hydrogen atoms attached to the  $\eta^2$ -bound carbons were placed on the basis of a difference Fourier map for  $(\eta^5\text{-C}_5\text{Me}_5)\text{Rh}(\text{PMe}_3)(\eta^2\text{-phenanthrene})$ . The analogous hydrogen atoms for  $[(\eta^5\text{-C}_5\text{Me}_5)\text{Rh}(\text{PMe}_3)]_2(\mu\text{-}\eta^2\text{-}\eta^2\text{-C}_{10}\text{H}_8)$  were located in a similar manner, but the structure is not of such a high quality, and so the hydrogen atom positions are less reliable (Jones, W. D., personal communication).

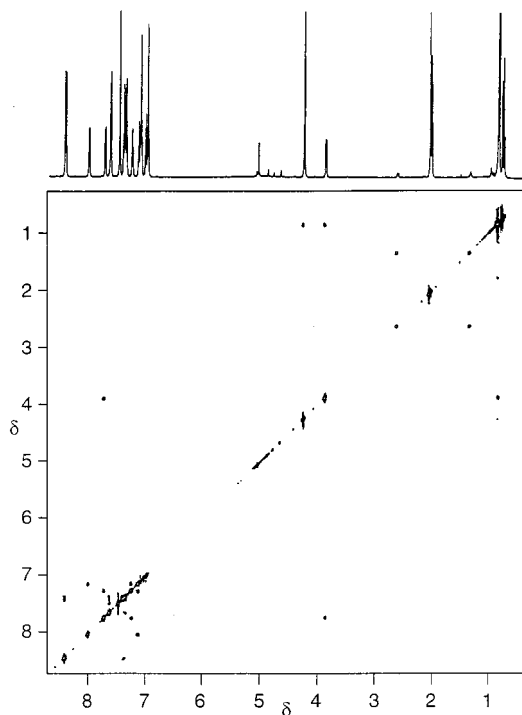
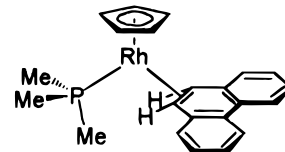


**Figure 7.**  $^1\text{H}$ – $^1\text{H}$  NOESY spectrum of  $(\eta^5\text{-C}_5\text{H}_5)\text{Rh}(\text{PMe}_3)(9,10\text{-}\eta^2\text{-phenanthrene})$  in  $d_8$ -toluene at 300 K (500.13 MHz,  $\tau_m = 1.6$  s, recycle delay = 4 s). All cross-peaks are of the NOE type.

**Scheme 4. Solution Structure of  $(\eta^5\text{-C}_5\text{H}_5)\text{Rh}(\text{PMe}_3)(9,10\text{-}\eta^2\text{-phenanthrene})$  from  $^1\text{H}$ – $^1\text{H}$  NOESY Studies**



spectrum was recorded at 300 K in  $d_8$ -toluene (recycle delay 20 s,  $\tau_m$  1.2 s) such that the spectrum is quantitative in terms of the phenanthrene and  $\text{PMe}_3$  resonances ( $5 \times T_1$ ) but involves a compromise for the  $\eta^5\text{-C}_5\text{H}_5$  resonance. As expected, there are no exchange cross-peaks. An NOE cross-peak is observed between the hydrogens attached to the  $\eta^2$ -bound carbon atoms ( $\text{H}^a$ ) and the  $\text{PMe}_3$  methyls, but no significant interactions are seen involving the ring. This spectrum indicates that the protons,  $\text{H}^a$ , are close in space to the  $\text{PMe}_3$  methyls, but not to the  $\eta^5\text{-C}_5\text{H}_5$  ring. Thus, the phenanthrene complex adopts a structure in solution analogous to the  $\eta^2$ -naphthalene complex (Scheme 4) and in agreement with the structure of the  $\eta^5\text{-C}_5\text{Me}_5$  analogue and  $(\eta^5\text{-C}_5\text{H}_5)\text{Rh}(\text{C}_2\text{H}_4)(9,10\text{-}\eta^2\text{-phenanthrene})$ .<sup>19,20,21f</sup>

Quantitative analysis of the NOESY spectrum follows the method established above (Table 4), making use of the rigid phenanthrene ring system for calibration of internuclear distances.<sup>43</sup> The results show the following.

(i) NOE interactions are detected only between nearest neighbor protons around the phenanthrene ring. The relative effective internuclear distances calculated from

(43) The partial overlap of the  $\text{H}^d$  resonance with one of the resonances of free phenanthrene made measurement of the on-diagonal peak intensity for  $\text{H}^d$  problematic. Similarly, accurate measurement of the  $\text{H}^c$  to  $\text{H}^d$  NOE cross-peak was difficult.

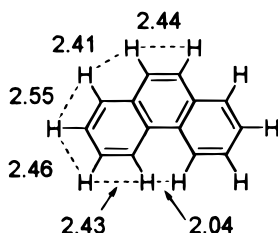


**Figure 8.** Average nonbonded internuclear distances within phenanthrene from neutron and X-ray diffraction data.<sup>44</sup>

the matrix analysis agree reasonably with the nonbonded internuclear distances within phenanthrene determined from X-ray and neutron diffraction measurements (compare Table 4 and Figure 8).<sup>44</sup>

(ii) By making use of the known distances separating neighboring phenanthrene hydrogens (Figure 8)<sup>44</sup> and relative  $r_{\text{eff}}$  values from Table 4, we estimate  $r_{\text{eff}}$  as 3.29 Å. From the X-ray crystal structure of  $(\eta^5\text{-C}_5\text{Me}_5)\text{Rh}(\text{PMe}_3)(\eta^2\text{-phenanthrene})$ , the corresponding distance is 3.43 Å, in reasonable agreement with the NOESY results (calculated using the  $1/\langle r^{-3} \rangle^{1/3}$  expression).

## Discussion

**1. NOESY Determination of Distances.** NOESY offers a simple method of obtaining structural and dynamic information for small organometallic complexes, and its use is likely to increase in the future. In the examples analyzed quantitatively, it was necessary to average the distances from nine methyl hydrogens to the arene hydrogens of interest. Comparisons with available X-ray data worked surprisingly well considering the likely errors in the NOE integrals and considering that the conformers present in solution may not be the same as those in the crystal. Moreover, the methyl hydrogens in the crystal structures had been placed at idealized locations. Use of the  $1/\langle r^{-3} \rangle^{1/3}$  factor also biases the average strongly toward conformers with shorter  $\text{H}\cdots\text{H}$  contacts.

**2. Exchange Phenomena in Naphthalene Complexes Studied by EXSY.** We have shown above that  $(\eta^5\text{-C}_5\text{H}_5)\text{Rh}(\text{PMe}_3)(\eta^2\text{-naphthalene})$  undergoes exchange of  $\text{H}^1$  and  $\text{H}^2$  with  $\text{H}^4$  and  $\text{H}^3$ , respectively, with  $\Delta G^\ddagger_{300} = 74.4 \text{ kJ mol}^{-1}$ . A similar linkage isomerization process has recently been reported for  $(\eta^5\text{-C}_5\text{Me}_5)\text{Ru}(\text{NO})(\eta^2\text{-1,2-C}_{10}\text{H}_8)$ .<sup>22</sup> In this system, cooling is required to see sharp, coupled resonances. By contrast, the  $(\text{Pr}_2\text{P}(\text{CH}_2)_n\text{P}(\text{Pr}_2)\text{-Ni}(\eta^2\text{-C}_{10}\text{H}_8)$  ( $n = 2, 3$ ) complexes have been shown by solid-state and solution  $^{13}\text{C}$  NMR studies to be highly fluxional.<sup>45</sup> Solid-state magnetization transfer experiments indicate the occurrence of an exchange process analogous to those described above.<sup>45</sup> The  $^{13}\text{C}$  NMR spectra in solution reveal three fluxional processes for the Ni complexes. The activation energy,  $\Delta G^\ddagger$ , for exchange between C(1)/C(4) and C(2)/C(3) was calculated to be approximately  $25 \text{ kJ mol}^{-1}$ , and the transition state is proposed to be an  $\eta^4$ -coordinated species

(16-electron  $\eta^2$ -coordination to 18-electron  $\eta^4$ -coordination). In a second, higher energy exchange process ( $\Delta G^\ddagger \approx 63 \text{ kJ mol}^{-1}$ ), the Ni center migrates onto the other naphthalene ring (1,2 to 8,9 shift) and the phosphines become equivalent. A third fluxional process of similar activation energy ( $\Delta G^\ddagger \approx 54 \text{ kJ mol}^{-1}$ ) involves rotation of the naphthalene ligand about the  $\text{Ni}-\eta^2\text{-CC}$  axis, analogous to the "propeller" rotation seen for coordinated alkenes.

In his recent review, Harman presents a summary of the rates of linkage isomerization for a variety of  $[\text{Os}(\text{NH}_3)_5(\eta^2\text{-arene})]^{2+}$  complexes.<sup>24</sup> For  $[\text{Os}(\text{NH}_3)_5(\eta^2\text{-C}_6\text{H}_6)]^{2+}$ , the rate constant is extremely fast,  $k = 1 \times 10^4 \text{ s}^{-1}$  at 290 K. For the isomerization of  $[\text{Os}(\text{NH}_3)_5((3,4\text{-}\eta^2)\text{-1-methylnaphthalene})]^{2+}$  across the ring junction to  $[\text{Os}(\text{NH}_3)_5((5,6\text{-}\eta^2)\text{-1-methylnaphthalene})]^{2+}$ , the rate is very slow,  $k = 2 \times 10^{-6} \text{ s}^{-1}$ .<sup>21h,24</sup> For the intraring isomerization for  $[\text{Os}(\text{NH}_3)_5(\eta^2\text{-subst. naphthalene})]^{2+}$  complexes (where subst. naphthalene = 1-methylnaphthalene, 2-methylnaphthalene, 2-methoxynaphthalene, and 2-hydroxynaphthalene), Harman suggests that  $k$  lies in the range  $10^{-3}$  to  $1 \text{ s}^{-1}$ . Thus, the rate for the 1,2 to 3,4 shift in  $(\eta^5\text{-C}_5\text{H}_5)\text{Rh}(\text{PMe}_3)(\eta^2\text{-C}_{10}\text{H}_8)$  of  $(3.5 \pm 0.1) \times 10^{-1} \text{ s}^{-1}$  is in line with Harman's findings for an intra-ring isomerization.

## Conclusion

NOESY experiments have demonstrated that  $(\eta^5\text{-C}_5\text{H}_5)\text{Rh}(\text{PMe}_3)(\eta^2\text{-C}_{10}\text{H}_8)$  adopts a structure in solution with the bonds to the hydrogens on the  $\eta^2\text{-C}=\text{C}$  atoms bent out of the arene plane, away from the  $\eta^5\text{-C}_5\text{H}_5$  ligand. From the cross-relaxation rates,  $\sigma_{ij}$ , the effective through-space distance between  $\text{H}^1$  (or  $\text{H}^2$ ) and the  $\text{PMe}_3$  hydrogen atoms was found to be ca. 7–5 times the distance from  $\text{H}^1$  to  $\text{H}^8$ . The effective  $\text{H}^1$  (or  $\text{H}^2$ ) to  $\text{PMe}_3$  hydrogen separation,  $r_{\text{eff}}$ , was calculated as 3.52 Å from the NOESY data.

There is an equilibrium between  $(\eta^5\text{-C}_5\text{H}_5)\text{Rh}(\text{PMe}_3)(\eta^2\text{-C}_{10}\text{H}_8)$  and the C–H activation product,  $(\eta^5\text{-C}_5\text{H}_5)\text{-Rh}(\text{PMe}_3)(\text{C}_{10}\text{H}_7)\text{H}$ . The free energy change for the conversion from  $\eta^2$ -naphthalene to (naphthyl)hydride complex,  $\Delta G^\circ_{300}$ , is  $+11.5 \text{ kJ mol}^{-1}$ . A similar equilibrium is observed for the  $\eta^5\text{-C}_5\text{Me}_5$  system. The difference in free energy for the equilibria,  $\Delta\Delta G^\circ_{300}$ , is  $-9.3 \text{ kJ mol}^{-1}$  (defined as  $\{\Delta G^\circ_{300}(\eta^5\text{-C}_5\text{Me}_5) - \Delta G^\circ_{300}(\eta^5\text{-C}_5\text{H}_5)\}$ ). Quantitative comparisons of energetics between  $\eta^5\text{-C}_5\text{Me}_5$  and  $\eta^5\text{-C}_5\text{H}_5$  complexes are unusual.

An intramolecular [1,3]-shift process moves the site of Rh- $\eta^2$ -coordination in  $(\eta^5\text{-C}_5\text{H}_5)\text{Rh}(\text{PMe}_3)(\eta^2\text{-C}_{10}\text{H}_8)$  from one side of the ring to the other (C(1)–C(2) to C(3)–C(4)). There is no evidence for migration onto the uncoordinated ring. From EXSY experiments, the rate of the exchange process was determined as  $(3.5 \pm 0.1) \times 10^{-1} \text{ s}^{-1}$  at 300 K and  $\Delta G^\ddagger_{300}$  as  $74.4 \text{ kJ mol}^{-1}$ .

X-ray diffraction demonstrates that  $[(\eta^5\text{-C}_5\text{H}_5)\text{Rh}(\text{PMe}_3)]_2(\mu\text{-}\eta^2\text{-}\eta^2\text{-C}_{10}\text{H}_8)$  adopts an *antifacial*- $\mu\text{-1,2-}\eta^2\text{-3,4-}\eta^2$  arrangement, with the hydrogen atoms on the  $\eta^2$ -bound carbons distorted out of the plane of the naphthalene ligand. NOESY studies on the dimer suggest that the same structure is adopted in solution and give the mean value of  $r_{\text{eff}}$  as 3.48 Å. From the X-ray crystal

(44) Kay, M. I.; Okaya, Y.; Cox, D. E. *Acta Crystallogr.* **1971**, B27, 26.

(45) Benn, R.; Mynott, R.; Topalovic, I.; Scott, F. *Organometallics* **1989**, 8, 2299.

structure, the mean distance in the solid state is calculated as 3.56 Å.

Thermal reaction of  $(\eta^5\text{-C}_5\text{H}_5)\text{Rh}(\text{PMe}_3)(\text{C}_6\text{H}_5)\text{H}$  with phenanthrene yields the symmetrically bound phenanthrene complex,  $(\eta^5\text{-C}_5\text{H}_5)\text{Rh}(\text{PMe}_3)(\eta^2\text{-9,10-C}_{14}\text{H}_{10})$ . NOESY studies show the same type of distortion as in the naphthalene complex. The value of  $r_{\text{eff}}$  measured by NOESY is 3.29 Å. The corresponding distance from the X-ray crystal structure of  $(\eta^5\text{-C}_5\text{Me}_5)\text{Rh}(\text{PMe}_3)(\eta^2\text{-9,10-phenanthrene})$  is 3.43 Å.

**Acknowledgment.** We appreciated valuable discussions with Dr. S. B. Duckett, Professor W. D. Jones, and Dr. B. Messerle. We acknowledge the support of EPSRC.

**Supporting Information Available:** Crystallographic data for  $[(\eta^5\text{-C}_5\text{H}_5)\text{Rh}(\text{PMe}_3)]_2(\mu\text{-1,2-}\eta^2\text{-3,4-}\eta^2\text{-C}_{10}\text{H}_8)$ . This material is available free of charge via the Internet at <http://pubs.acs.org>.

OM9908377